FASTER THAN NYQUIST SIGNALING BASED ON ENERGY SPREADING TRANSFORM AND IDEAL ENERGY SPREADING TRANSFORM

A Thesis
Presented to
The Academic Faculty

by

Juho Lim

In Partial Fulfillment
of the Requirements for the Degree
Master of Science in the
School of Electrical and Computer Engineering

Georgia Institute of Technology
August 2016

FASTER THAN NYQUIST SIGNALING BASED ON ENERGY SPREADING TRANSFORM AND IDEAL ENERGY SPREADING TRANSFORM

Approved by:

Professor Geoffrey Ye Li, Advisor
School of Electrical and Computer Engineering
Georgia Institute of Technology

Professor David V Anderson
School of Electrical and Computer Engineering
Georgia Institute of Technology

Professor Magnus Egerstedt
School of Electrical and Computer Engineering
Georgia Institute of Technology

Date Approved: 1 July 2016

To my parents.,

Thank you

ACKNOWLEDGEMENTS

First and foremost, I would like to especially thank my mother, father and families, without whose guidance and support I would not be here. Besides, I would like to present my sincere gratitude to Prof David V Anderson, Throughout my times at Georgia Tech, I got valuable advice and help from him.

I also appreciate the kindness of all lab members of Information Transmission and Processing Laboratory (ITP Lab) who gave me lots of help on my research and Prof Magnus Egerstedt and Geoffrey Ye Li. Their feedback are always valuable for my research and helped me to get a better opportunities.

TABLE OF CONTENTS

LIST OF TABLES

LIST OF FIGURES

SUMMARY

The objective of this thesis is to develop a modulation and demodulation scheme which is based on Iterative Decision Feedback Equalization and can be applied to Faster than Nyquist Signaling (FTNS) with low complexity and high numerical stabilities.

FTNS is a way to increase the data rate by giving up orthogonal condition in both domains. But FTNS increases demodulation complexity and instability at the expense of high data rate. Especially, the complexity of Maximum Likelihood Sequence Detection (MLSD), which is the near-optimal method of Nyquist Signaling scheme, is not tractable in FTNS.

We propose a FTNS scheme grounded on Energy Spreading Transform (EST) based Iterative Decision Feedback Equalization (IDFE). EST based IDFE consists of EST and IDFE and was originally proposed by Hwang [15] for frequency selective channel problem. The complexity of EST based IDFE is fixed and it is robust to parameter estimation error.

In this thesis, we analyze couple of interesting properties of EST and find a way to enhance internal IDFE performance. Then we simulate robustness and performance of the proposed FTNS scheme in different conditions and compare the results to other recently proposed FTNS schemes.

CHAPTER I

INTRODUCTION

Developing a Faster-than-Nyquist Signaling (FTNS) system with low complexity and high performance by using Iterative Decision feedback equalizer is the objective of this research. We used Energy Spreading Transform (EST) for FTNS and revealed couple of the mathematical properties of EST. The concept of FTNS problem and the proposed solution will be explained.

1.1 Motivation

Telecommunication researches are divided into multiple layers. Among them, physical layer problems are the most heavily researched and mature then other layer problem. Especially, when it comes to the simple telecommunication cases ,such as stationary one to one wide-band communication in free space, people already had nearly reached theoretical performance bound called channel capacity in early 90's.

Therefore, nowadays researchers are focusing on more complex cases , such as MIMO, Mobile communication, or other higher layer topics. But I would like to enhance the telecommunication performance by tackling basic condition widely assumed in many other telecommunication researches.

The condition we gave up in this thesis is orthogonality condition. In modern telecommunication, modulation pulses are orthogonal to each other either in time domain or in frequency domain. For instances, the down-link scheme of Long Term Evolution (LTE) is Orthogonal Frequency Division Modulation (OFDM) and the up-link scheme of LTE is Single-carrier (SC) Nyquist Signaling. In these two schemes modulation pulses are overlapped in either frequency domain (OFDM) or time domain (Nyquist Signaling)but orthogonal to each others.

What people focuses on first is Nyquist Signaling condition. Nyquist Signaling has been widely adopted in many researches and protocols for a long time. Because the channel in Nyquist Signaling can be simplified in discrete time domain. But giving up Nyquist Signaling and introducing additional complexity enhance the transmission rate without increase of error rate. This was found by J.E Mazzo in 1975. He showed that sending signal faster than Nyquist rate does not increase error rate in some condition [20]. It is called Faster Than Nyquist Signaling (FTNS).

However using the near optimal NS demodulation method, Maximum-likelihood Sequence Detection (MLSD), for FTNS demodulation grows its complexity exponentially. Equalization based demodulation methods are alternatives of MLSD methods. Among them, Frequency domain equalizers (FDE) have less complexity. And Energy Spreading Transform (EST) based Iterative Decision Feedback Equalizer (IDFE) is one of FDE which has shown good performance in frequency selective channel.

In this thesis, we will reformulate FTNS problem similar to the that of the frequency selective channel problem and apply EST based IDFE. I also investigate ways to enhance EST based IDFE performance and to extend it to other equalizers by analyzing its properties.

1.2 Thesis Organizations

The remaining contents of this thesis is organized as follows.

1 In Chapter 2, brief reviews on required communication backgrounds are presented. First, the definition of Nyquist Signaling is explained. Then, I will explain two most widely used discrete time channel models. These model simplify all continuous time events between modulation and demodulation and allow us to formulate FTNS problem in discrete time domain. Lastly, brief explanation of Cyclic Extension is presented.

2 Chapter 3 explain the definition of FTNS and difficulties of using FTNS. It

explores the previous researches on FTNS.

3 *Energy Spreading Transform* (EST) based *Iterative-decision-feedback equalization* (IDFE) is reviewed in this Chapter 4. I first explain the concept of IDFE. Secondly, How EST enhance IDFE performance is discussed.

4 In chapter 5, we investigate EST based IDFE more in depth. I applied EST to varieties of IDFEs and checked which one show the best performance. How the infrequent filter update rule can enhance the performance of IDFEs is discussed in the next section. Additionally, we propose the first ideal EST and analyze couple of mathematical properties of EST.

5 Chapter 6 apply EST based IDFE, in chapter 5, to FTNS. First we explain the discrete time channel model we use and things should be changed for EST based IDFE to be applied to FTNS. Lastly, we will see the simulation results of the proposed FTNS scheme and how robust it is to the difficulties of FDE bassed FTNS we saw in chapter 3.

1.3 Notation and Abbreviations

Through out this paper, we note vector in bold small letters as $\mathbf{x}$ and matrix in bold capital letter as $\mathbf{X}$. $\mathcal{F}(\cdot)$ and $\mathcal{E}(\cdot)$ is the Fast Fourier Transform and the Energy-Spreading-Transform. We will use big capital letter for Discrete Fourier Transform (DFT) coefficients of vector $\mathbf{x}$, $X_k = \mathcal{F}_k(\mathbf{x})$. Lower subscription n in x_n means n th element of vector $\mathbf{x}$. Upper subscription i in $\mathbf{x}^{(i)}$ means i th iteration on vector $\mathbf{x}$.

CHAPTER II

COMMUNICATION BACKGROUND

2.1 Nyquist Signaling

Nyquist signaling is one of the most basic assumptions of most time domain telecommunication. Sending signal through the linear modulation of T-orthogonal pulses in Nyquist rate T which satisfy zero-crossing criterion is called Nyquist signaling. T-orthogonal pulses are orthogonal to their T times shifted copies. Zero-crossing criterion means all neighboring pulses cross zero when the target pulse (blue) is sampled at $t = 2$ as 1.

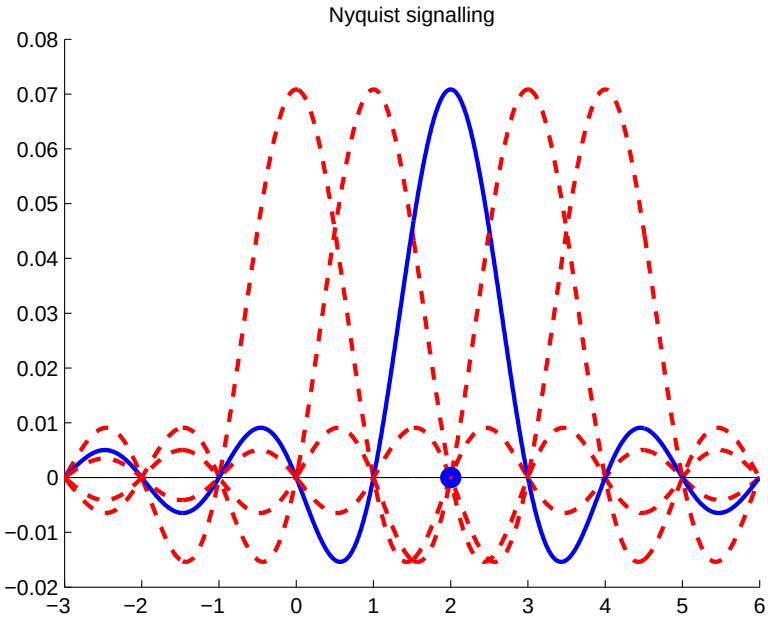

Figure 1: Nyquist Signalling

Therefore Nyquist signaling guarantees free inter-symbol-interference (ISI) condition in wide band channel. ISI is a interference from forwarding or backwarding symbols which can be expressed in convolution operation. The wide band channel

means that there are no external issues ,such as multi-path, which entail ISI. This free ISI condition of Nyquist Signaling is preferred because it makes demodulation and detection complexity of receiver side simple.

To sum up, received symbols, $\mathbf{r}$, through the Nyquist Signaling in wide band channel is the sum of actual symbol value, $\mathbf{s}$, with additive white Gaussian noise, $\mathbf{w}$,.

$$\mathbf{r} = \mathbf{s} + \mathbf{w} \tag{1}$$

In narrow band channel, ISI is entailed and thus the channel impulse response $\mathbf{h}$ become not one.

$$\mathbf{r} = \mathbf{h} * \mathbf{s} + \mathbf{w} \tag{2}$$

The actual communication happens in continuous time domain.

2.2 Discrete time channel models

Discrete time channel models,1 and 2, are simplified expression of the single carrier linear modulation scheme. There are two well known : Forney model and Ungerboeck model. The definition of these two models are presented in this chapter which will help you to understand the origin of main difficulty in FTNS .

Consider signal generated by transmitter through the Nyquist Signalling.

$$g(t) = \sum_{n=1}^{N} s_n \psi(t - nT) \tag{3}$$

$\mathbf{s} = [s_1, s_2, \cdots, s_N]$ is symbol vector and each s_i has complex value limited in finite signal space. $\psi(t)$ is any T-orthogonal pulse. In AWGN channel, what receiver received is

$$r(t) = h(t) * g(t) + w(t) \tag{4}$$

If channel is wideband, $h(t)$ is delta function $\delta(t)$. To maximize Signal-to-Noise Ratio (SNR), the received signal $r(t)$ is filtered by the matched filter $m(t) = h(-t)^* * \psi(-t)^*$ and then is sampled.

$$y_n^{Ung} = \big(m(t) * r(t)\big)|_{t=nT} \tag{5}$$

The equation (6) is the simplified channel notation between $\mathbf{s}$ and $\mathbf{y}^{Ung} = [y_1^{Ung}, y_2^{Ung}, \cdots, y_N^{Ung}]$. This is called Ungerbeock observation model.

$$\mathbf{y}^{Ung} = \mathbf{a} * \mathbf{s} + \boldsymbol{\mu} \tag{6}$$

$$\begin{aligned} \mathbf{a} &= \mathbf{h} * \mathbf{h}^{-*} * \boldsymbol{\psi} * \boldsymbol{\psi}^{-*} \\ \boldsymbol{\mu} &= \mathbf{h}^{-*} * \boldsymbol{\psi}^{-*} * \mathbf{w} \end{aligned} \tag{7}$$

Let us note $\mathbf{h}$ and ψ as T-sampled vectors of $h(t)$ and $\psi(t)$ and express conjugate mirror in as $-*$. $\mathbf{a}$ and $\mathbf{w}$ in are equivalent channel vector and noise vector.

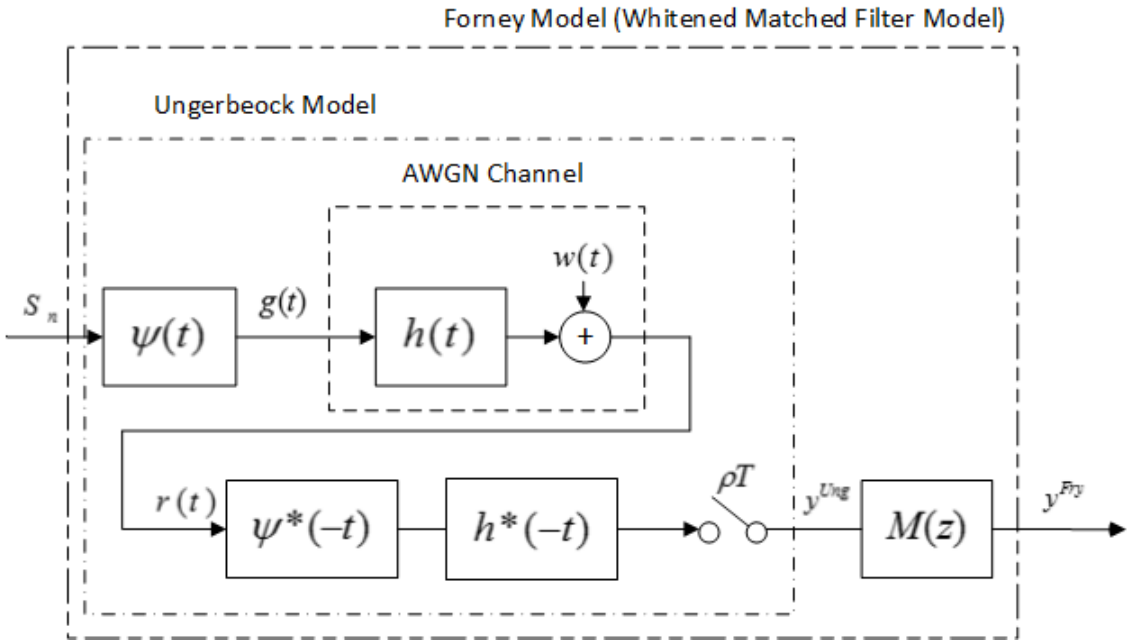

Figure 2: AWGN Channel Model

But in Ungerbeock observation model, the noise μ is not white. So noises are whitened additionally in Forney's model which is also called Whitened Matched Filter (WMF) model in equ 8. Whitening filter $\mathbf{m}$ is added to make the overall channel response $\mathbf{b} = \mathbf{m} * \mathbf{a}$ have minimum phase response. Thus $\mathbf{A}(z)$, $\mathbf{M}(z)$ and $\mathbf{F}(z)$, which are the inverse Z-transform of $\mathbf{a}$, $\mathbf{m}$, and the minimum phase components of

a, have a relationship described in equ 8.

$$\begin{aligned} \mathbf{A}(z) &= \gamma^2 \mathbf{F}(z)\mathbf{F}^*(1/z^*) \\ \mathbf{M}(z) &= \frac{1}{\gamma^2 \mathbf{F}^*(1/z^*)} \end{aligned} \tag{8}$$

γ is a separated gain factor in order to express $\mathbf{F}(z)$ as a monic function. Owing to the the Whitening filter, noise vector $\mathbf{w}$ becomes a white noise.

$$\mathbf{y^{Fry}} = \mathbf{b} * \mathbf{s} + \mathbf{w} \tag{9}$$

There is one advantage of Nyquist Signalling in these two model. $\mathbf{r}_{\psi\psi} = \psi * \psi^{-*}$ is a delta function because ψ is a sequence of nT sampled $\psi(t)$ and $\psi(t)$ is T-orthogonal. Thus, both Ungerbeock model channel $\mathbf{a}$ and Forney model channel $\mathbf{a}$ are further simplified in $\mathbf{h} * \mathbf{h}^{-*}$ and the minimum phase factor of $\mathbf{h} * \mathbf{h}^{-*}$. Since the numerical stabilities and complexities of demodulation algorithms depend on this two channel vectors $\mathbf{a}$, $\mathbf{b}$, modulation pulses do not increase stabilities and complexities of demodulation process in Nyquist Signalling.

For instances, the complexity of Maximum Likelihood Sequence Detection (MLSD) method, which is based on Forney's model, only depends on the length of $\mathbf{h}$. The numerical stabilities of Minimum Mean Square Error (MMSE) equalizer family are determined by frequency coefficients of $\mathbf{h}$.

2.3 Cyclic Extension and Frame-wise Frequency Domain Equalizer

The discrete time channel models we saw in previous section consist of linear convolution and addition operators. Suppose a transmitter send a symbol frame $\mathbf{s}$ through a multi-path channel in equation (10).

$$\mathbf{y} = \mathbf{b} * \mathbf{s} + \mathbf{w} \tag{10}$$

By inserting Cyclic Extension either in front of the frame or end of the frame, we can describe the linear convolution with $\mathbf{b}$ in terms of the circular convolution with $\mathbf{b}$ as

in equation ()13).

$$[\underbrace{x_{N-1-L_{cp}}, x_{N-L_{cp}}, x_{N-L_{cp}+1}, \cdots, x_{N-1}}_{\text{Cyclic Prefix}}, x_0, x_1 \cdots, x_{N-1}] \tag{11}$$

$$[x_0, x_1 \cdots, x_{N-2}, x_{N-1}, \underbrace{x_0, x_1 \cdots, x_{L_{CS}-1}}_{\text{Cyclic Suffix}}] \tag{12}$$

$$\mathbf{y} = \mathbf{b} \circledast \mathbf{s} + \mathbf{w} \tag{13}$$

Then circular convolution can be noted as a matrix multiplication.

$$\begin{aligned} \mathbf{y} &= \mathbf{B}\mathbf{s} + \mathbf{w} \\ &= \mathbf{F}^{*}\mathbf{\Sigma}_B\mathbf{F}\mathbf{s} + \mathbf{w} \end{aligned} \tag{14}$$

$\mathbf{B}$ is the circulant matrix of b and $\mathbf{\Sigma}_B$ is the diagonal matrix of the Fourier coefficient of b. And Fourier matrix, $\mathbf{F}$ is the Eigen-basis of circulant matrices. Thus all filtering operation can be processed by using Fast Fourier Transform (FFT). This is one of the common key idea of Frequency domain Equalizers.

CHAPTER III

LITERATURE REVIEW ON FTNS

In this chapter, the existing discussions on FTNS are presented. In first section, I explain the definition of FTNS and introduce theoretical proof and discussions for answering why FTNS is possible. Then I will explain the difficulties of using FTNS and introduce previous researches on this problem. Lastly, I reformulate FTNS problem and suggest two different approach in next two sections.

3.1 Definition of FTNS

In 1975, Mazzo published the first paper about *Faster Than Nyquist Signaling* (FTNS) [20]. In single-carrier FTNS, both following and followed pulses do not cross zero when the target pulse is sampled as in 3. Mazzo found that FTNS can increase spectral

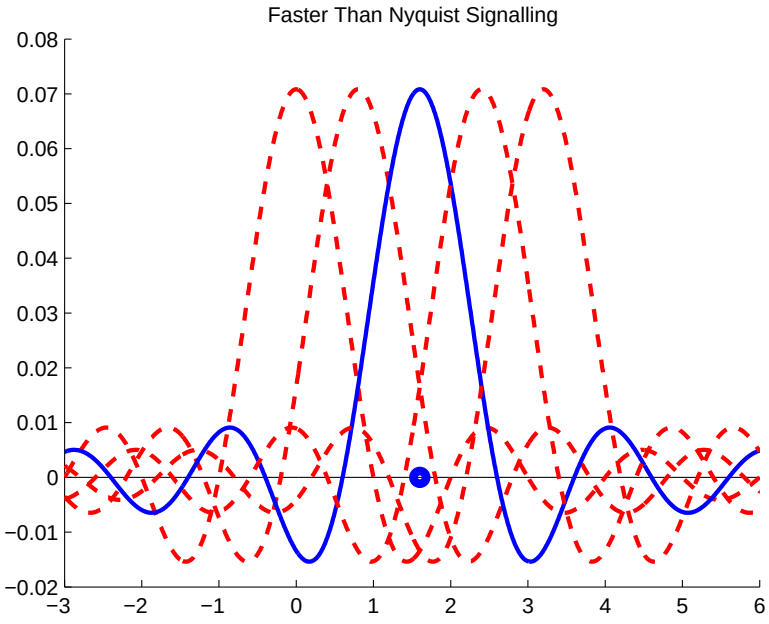

Figure 3: Faster Than Nyquist Signaling by 0.8

efficiency. Spectral efficiency is a performance index: bit/(s*Hz) which depends on Symbol error rate, symbol rate, and bandwidth.

3.1.1 Invariance of Minimum Distance

As we saw in 2.1, sending signal faster than Nyquist rate entails intrinsic-ISI and ISI typically increases symbol error rate (SER). The near-optimal SER one can achieves depends on the minimum distance between all the possible waveforms. Thus as long as minimum distance does not change symbol error rate does not increase [4].

Mazzo found that intrinsic-ISI, which is come form fast symbol rate above Nyquist rate, does not increases SER in some condition. He proved that the minimum distance of two different Binary Phase Shift Keying (BPSK) modulated waves is not reduced by the intrinsic-ISI from FTNS above 0.7. Later on the invariance of minimum distance in other signal constellation scheme such as QAM and other M-ary schemes are verified in [19].

3.1.2 Channel capacity of non-square PSD

It is an another interests whether the channel capacity of single-carrier FTNS is higher than that of Nyquist Signaling. Channel capacity, also referred as bit rate limit, is an performance bound, maximum bit rate one can achieve. In order to reach the channel capacity, channel coding should be applied. However, calculating the channel capacity, does not requires channel coding, so I will not deal with the concept of channel coding in this thesis.

Channel capacity depends on noise spectrum, channel spectrum and modulation pulse spectrum (waveforms). First we analyze free-ISI AWGN channel capacity. Let the unit power modulation pulses $\psi(t)$ have Power Spectrum Density (PSD) $S_{\psi\psi}(f)$ watts/Hz and the Noise power is N.

$$\int_0^\infty log_2(1 + \frac{S_{\psi\psi}(f)}{N/2})df \qquad \text{(bit/second)} \tag{15}$$

The equation 15 is the definition of channel capacity in AWGN channel. If modulation pulse has a fixed $[-W, W]$ bandwidth, 15 becomes

$$\int_0^W log_2(1 + \frac{S_{\psi\psi}(f)}{N/2})df \qquad \text{(bit/second)} \tag{16}$$

Equation (16) is called constrained information rate. When the bandwidth $[-W, W]$ and signal power $\int S_{\psi\psi}(f)df$ are fixed , spectral shape of ψ determines its information rate. This constrained information rate is maximized when the PSD $S_{\psi\psi}(f)$ has a rectangular shape as equation (17).

$$Wlog_2(1 + \frac{2P}{NW}) \qquad \text{(bit/second)} \tag{17}$$

The equation (refequ:ChCap) is the classical Shannon's Gaussian channel capacity.

The equation (17) is also traditionally used for non-sinc pulse as a benchmark. Instead of actual bandwidth W, 3dB cut-off frequencies, $W := W_{3db}$ are used for non-Since pulses to calculate equation 17. For instances, 3dB cut-off frequencies of Raised Cosine (RC) pulses are the same as that of the Sinc pulse which is W. Actually all T-orthogonal pulses have the same W_{3db} which is W is the actual bandwidth of Sinc pulse.

So despite of the fact that the actual bandwidth of RC pulses is $[-(1+\beta)W, (1+\beta)W]$, which larger than that of Sinc pulses, $[-W, W]$, the classical channel capacities of both Since pulse and RC pulses are same.

But the actual RC capacity calculated through the equation 15 is larger than the Sinc capacity in equation 18.

$$Wlog_2(1 + \frac{2P}{NW}) < \int_0^{W(1+\beta)} log_2(1 + \frac{S_{\psi\psi}(f)}{N/2})df \tag{18}$$

In [24], [18], Rusek and Anderson insist that FTNS can utilize this extra bandwidth which is not considered at the classical channel capacity. They showed that the right hand side of 18 always increase as β grows up, and assert that better codes can be assembled in 15.

3.1.3 Series of FTNS

We have seen the definition and motivation of time domain FTNS. And the same concept can be applied to frequency domain FTNS. Orthogonal Frequency Division Modulation (OFDM) is the comparable modulation scheme which satisfies zero-crossing criterion in frequency domain as Nyquist Signaling satisfies it in time-domain. Thus time-domain FTNS analysis can be directly applied to frequency domain FTNS [23]. We will stick to time domain FTNS in this thesis.

3.2 Difficulties of using Conventional model to FTNS

We observed two different ways of validating theoretical possibility of FTNS in previous section. In this section, we reformulate FTNS problem in a discrete time channel model which is similar to others in 2.2.

We had seen that the overall channel response vector of Ungerbeock model and WMF model: $\mathbf{a}$ of the equation 6 and $\mathbf{b}$ of the equation 9 in section 2.2, only depend on the external channel $\mathbf{h} = h(nT)$, because $\mathbf{r}_{\psi\psi}$ is a Kronecker delta function in Nyquist Signaling as the following equations.

$$r_{\psi\psi}(t) = \int_{-\infty}^{\infty} \psi(\tau - t)\psi^*(-\tau)d\tau \tag{19}$$

$$\mathbf{r} = \boldsymbol{r_{\psi\psi}(n\rho T)} = \boldsymbol{\psi} * \boldsymbol{\psi}^{-*} \tag{20}$$

where $r_{\psi\psi}(t)$ is correlation function of modulation pulse ψ and $\mathbf{r}_{\psi\psi}$ is ρT sampled $r_{\psi\psi}(t)$. Since $\psi(t)$ is T-orthogonal, $r_{\psi\psi}(t)$ becomes a $\delta(t)$ when we set $\rho = 1$ (Nyquist signaling).

But in FTNS, ρ is less than 1. Therefore $\mathbf{r}_{\psi\psi}$ is not a delta function in FTNS, because $\psi(t)$ does not cross zero in $n\rho T$ points for $\rho < 1$ as figure 4. As a result, not only $\mathbf{h}$ but also $\mathbf{r}_{\psi\psi}$ should be considered for calculating channel vectors $\mathbf{a}$ and $\mathbf{b}$ and noise vector μ. And couple of difficulties of using FTNS are grounded on some characteristics of $\mathbf{b}$.

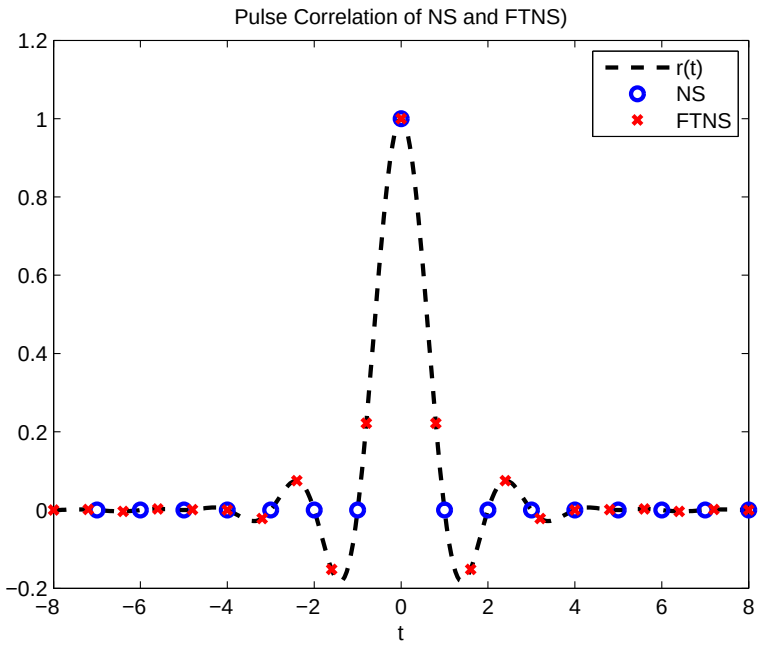

Figure 4: r(t) and sampled its sampled vector in 0.8 FTNS and NS

- **Unable to use Whitened Matched Filter Model**

  First, due to the null-frequency response of the noise vector μ, the noise can not be whitened and it is impossible to use WMF model in FTNS. Let us analyse the frequency response of μ. According to the equation (7), amplitude spectrum of noise vector μ is the square root of amplitude spectrum of $\mathbf{a}$. For simplicity, we will assume $\mathbf{h} = 1$ which change the Ungerbeock channel $\mathbf{c}$ as $\mathbf{a} = \mathbf{r}_{\psi\psi}$. Let's see frequency responses of four $\mathbf{r}_{\psi\psi}$ in four different FTNS to check why it is impossible to make a filter canceling maximum phase components of $\mathbf{r}_{\psi\psi}$. In fig 5, symbol rate of the blue lines are 67% ($\rho = 0.6$) faster than NS and that of the red lines are 25% ($\rho = 0.8$) faster than NS. As a reminder, β is roll-off factor which determine pulse decay rate and extra bandwidth.

  $\mathbf{r}_{\psi\psi}$ is like a low-pass filters whose 3db cut-off frequency is at $\rho \cdot \pi$. And transition regions depend on β. As β decrease, high frequency coefficients in $[\rho\pi, \rho\pi]$ and $[-pi - \rho * \pi]$ rapidly go to zeroes. Thus if the symbol rate becomes higher

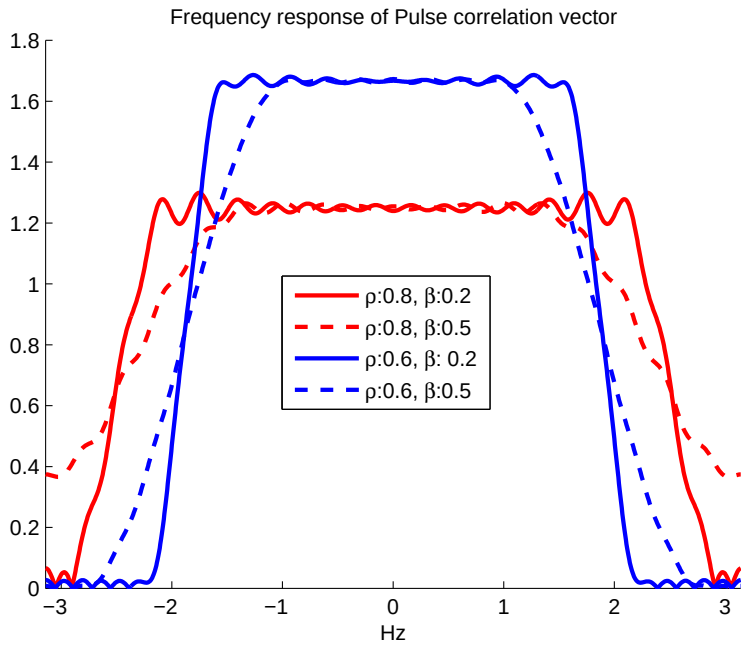

Figure 5: Frequency Response of $\mathbf{r}_{\psi\psi}$ in FTNS

(ρ becomes lower) or the roll-off factor β of $\psi(t)$ becomes lower (Bandwidth becomes narrower), the null frequency regions in high frequency band becomes wider. In other word, FTNS increase dynamic range of frequency coefficients of $\mathbf{r}_{\psi\psi}$. Because, null frequency component not only means the coefficients whose values are zeros but also means that some of coefficients are relatively too smaller than the others.

If $\mathbf{m}$ exists, the amplitude of its frequency coefficients are proportional to the reciprocal of frequency coefficients of $sqrt(\mathbf{r}_{\psi\psi})$. Since the frequency coefficients of $sqrt(\mathbf{r}_{\psi\psi})$ are nearly zeros, the corresponding frequency coefficients of $\mathbf{m}$ become infinite, which means that $\mathbf{m}$ is numerically unstable. Thus, the derived $\mathbf{m}$ can not whiten the noise spectrum $\mathbf{w}^*\psi$, where $\mathbf{w}$ and ψ are the sampled noise vector and the modulation pulse.

Therefore it is impossible to whiten the noise spectrum which has null frequency components and whitening filter $\mathbf{m}$ in defined in equ 8 of 2.2 can not whiten

the output of Ungerceock model. WMF model can not be derived in FTNS.

- **Long Channel Response**

  Secondly, longer response of $\mathbf{r}_{\psi\psi}$ in FTNS increases MLSD demodulation complexity. The complexity of MLSD method depends on the length of channel vector $\mathbf{a}$. Let us note lengths of $\mathbf{a}$, $\mathbf{h}$ and $\mathbf{r}_{\psi\psi}$ are N_a, N_h and N_r. Then, $\mathbf{a}$ is

  $$N_a = N_r + 2 \cdot N_h - 2 \tag{21}$$

  In NS, N_r is one because it is a sampled delta function. But in FTNS, the length of $\mathbf{r}_{\psi\psi}$ is proportional to modulation pulse $\psi(t)$ duration when the pulse duration is finite. For example, in FTNS with $\rho = 0.7$ and 6 pulse duration $\psi(t)$, N_r becomes $15 = \lceil 12/0.8 \rceil$. Thus as pulse duration and FTNS rate increase, N_a becomes larger.

  Now, I will briefly explain what is MLSD demodulation method and why large N_a increase its complexity. In MLSD method, symbol vector $\mathbf{s}$ is treated as an state transition trajectory in Markov chain. Previously received N_a symbols are represented as a state. Thus the number of states in each transition is M^{N_a} and the next state is determined by $s[N_a+1]$ symbol. Under this scheme, in order to demodulate a size L frame M-ary symbol vector received through the channel with length N_a channel memory, receiver need to calculate size M^{N_a} transition matrix by L times. Therefore, MLSD complexity increases exponentially as N_a increases and MLSD is too expensive to use when channel vector is long.

  Furthermore, pulse durations of FTNS simulations are generally longer than that of NS. In [1, 19, 21, 22], researchers used a 40 duration modulation pulse which makes $N_r > 100$. Thus M^{N_a} in FTNS is far larger than M^{N_a} in NS. Calculating non-sparse M^{100} square matrix is impossible.

To sum up, we can not use WMF model in FTNS and MLSD is too expensive to use in FTNS.

3.3 Approximated Maximum-likelihood-sequence-detection

The most widely used demodulation method in single-carrier (SC) linear pulse coded modulation (PCM) scheme is MLSD method based on WMF model [11]. Because Maximum-likelihood-sequence-detection (MLSD) guarantees near-optimal solution for SC linear modulation and it can be jointly implemented with decoder, like turbo-equalization. Researchers have proposed some way to overcome the difficulties of using MLSD to FTNS we saw in previous section: WMF model can not be derived, and the number of branch metric need to be computed in MLSD of FTNS are too large. [19]

First problem can be resolved by using the MLSD methods based on Ungerbeock model [30]. Unlike WMF model, branch metrics (state transition matrix) of Ungerbeock MLSD can be calculated without white noise assumption because Noise covariance matrix is considered in calculating branch metrics.

For the second complexity problem, several modified-MLSD algorithms are proposed. JB Anderson applied M-BCJR [12], which is one of reduced-trellis MLSD methods, to FTNS [2]. Instead of calculating all branch metrics which are elements of size M^{N_a} transition matrix, the algorithm only consider M_t largest states, it first truncates the number of current states into $M_t << M^{N_a}$, then it only calculates $M_t \times (M_t \cdot M)$ branch metrics which are far less than $M^{N_a} \times M^{N_a}$.

Also numerical simulation showed that this truncated trellis MLSD [3] works well in Ungerbeock model than WMF model which can not apply to FTNS.

3.4 Equalization methods

Using Equalization is a way to avoid this complexity issues. Unlike MLSD approaches, the complexities of linear equalization methods do not increase exponentially when channel memory increase. Moreover, the complexity of Frequency Domain Equalizers

are not effected by channel memory at all because their computation are conducted in frequency domain through FFT.

Recently, several FDE solutions for FTNS were suggested. Shinya et all [27] propose CP extension with minimum mean square error (MMSE) turbo equalizer, and Tomasin et all suggest fractionally sampled Iterative Block Decision Feedback Equalizer (IBDFE) method with LDPC code [29], [28].

Although the equalization methods have much lower complexities than MLSD approaches, they also have some demerits such as channel estimation error, colored noise and numerical stability. Fukumoto [13] designed a scheme which are free of the channel estimation error from modeling assumption. Gattami [14] and Chen [9] suggest modulation pulse schemes which reduces the issues above.

In this paper, we will propose a EST based FDE scheme whose structure is similar to that of these two [29], [27] but has better performance and robustness.

3.5 Summary

In this chapter, we checked the definition of FTNS and the difficulties of using FTNS. Due to the high complexity of MLSD, equalization methods are more attractive in FTNS. But the equalization methods also have some problems. We will see more detailed difficulties of using equalization technique in FTNS in chapter 6.

CHAPTER IV

LITERATURE REVIEW ON EST AND IDFE

This chapter aims at explaining *Energy Spreading Transform* (EST) and *Iterative Decision Feedback Equalization* (IDFE) demodulation method. We will review IDFE in first section 4.1 then EST in the next section 4.2. Because EST is an add-on algorithm for IDFE methods, which enhance IDFE performance. One thing we should note here is that we used $\mathbf{a}$ and $\mathbf{b}$ as the coefficient vectors of filters while they were Ungerbeock and Forney channel vectors in the previous sections.

4.1 Iterative Decision Feedback Equalizer (IDFE)

IDFE is a non-linear frequency domain equalizer which is applied to the block-wise discrete time channel schemes

$$\mathbf{y} = \mathbf{c} \circledast \mathbf{x} + \mathbf{w} \tag{22}$$

where $\mathbf{x}$, $\mathbf{c}$, $\mathbf{y}$, and $\mathbf{w}$ are transmitted signal, channel vector, received signal and noise vector. IDFE is motivated to overcome drawbacks of Decision Feedback Equalizer (DFE). DFE cancels ISI by using previously detected symbols [4]. But it has error propagation problem: incorrectly determined previous symbol affect the next symbol decisions. Also DFE can not cancel post-cursor ISI [7].

IDFEs are block(frame)-wise equalization methods to solve these limits. IDFE decides whole symbols in the received frame at once, while DFE decides each symbol in the frame one by one. IDFE repeats the equalization task on the same set of received frame iteratively till the determined symbol frame converges. There are several variations of Iterative Decision Feedback Equalizers (IDFE). Among them, the EST based IDFE [16] is grounded on the two equalizers suggested in [7] and [5].

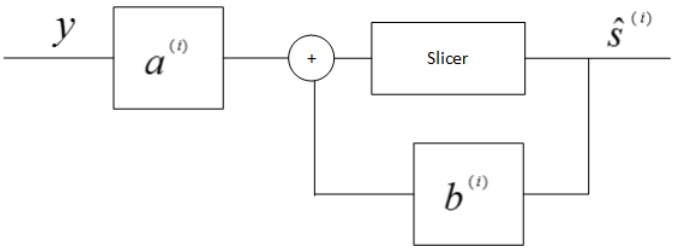

Figure 6: Hard-decision IDFE

IDFE consists of two equalizers: Feed-Forward (FF) filter , $\mathbf{a}$, and FeedBack (FB) filter, $\mathbf{b}$, in Figure (6). Thus , depending on types of FF and FB filter pairs, varieties of IDFEs can be designed.

Among them, Equalizers in [6, 7, 10, 25] consist of two linear equalizer (LE) pair. One merit of LE is that filtering can be computed by modulation in frequency-domain instead of convolution in time-domain. Then their overall complexity become only the order of $\mathcal{O}(NlogN)$ which come from Fast Fourier Transform (FFT). In order to use block wise FFT filtering, Cyclic Extension should be inserted at the begin or end of the frame.

Typically FB filter $\mathbf{b}^{(i)}$ is intuitively chosen to cancel interference terms in $\mathbf{a}^{(i)} * \mathbf{c}$. Then the expected error energy (cost function) can be represented as a function of FF filter $\mathbf{a}^{(i)}$ and the symbol vector decided in previous iteration $\hat{\mathbf{s}}^{(i)}$. The next FF filter $\mathbf{a}^{(i+1)}$ is chosen to minimize error energy.

$$\begin{aligned} \min_{\mathbf{a},\mathbf{b}} \parallel \mathbf{s} - \left(\mathbf{a} \circledast \mathbf{y} - \mathbf{b} \circledast \hat{\mathbf{s}}\right) \parallel \\ \text{s.t. } \mathbf{b} = \mathbf{a} * \mathbf{c} - \delta \end{aligned} \tag{23}$$

Most of IDFE papers share this common idea. More detailed derivation of general IDFE is in [6].

4.2 Energy Spreading Transform

Energy Spreading Transform (EST), proposed by Hwang in [15], makes IDFE robust to the localized errors I mentioned in the previous section.

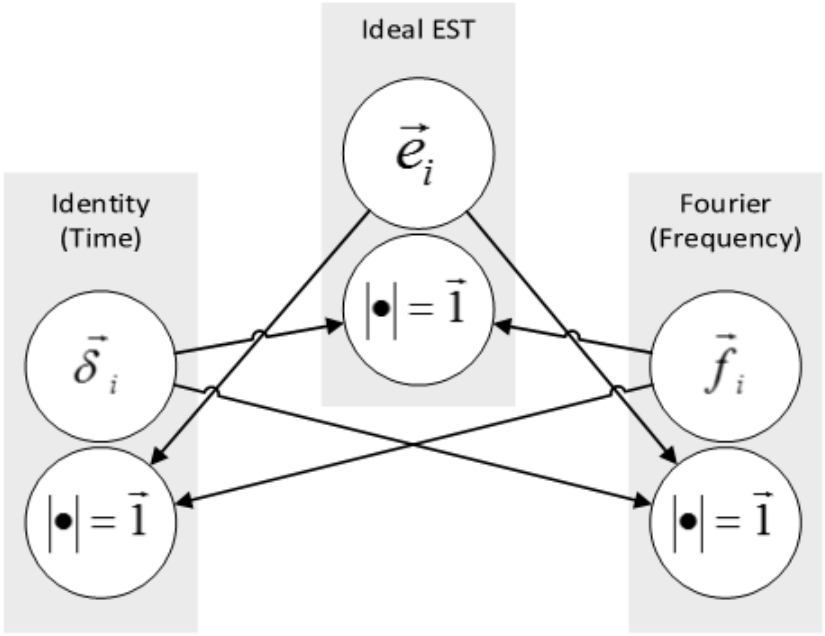

Figure 7: Transform Relationship between Identity, Fourier and Ideal EST

4.2.1 Definition

EST is a block-wise linear transformation which can be expressed as an matrix multiplication. So EST of $\mathbf{s}$ is defined as an matrix multiplication, $\mathcal{E}(\mathbf{s}) = \mathbf{Es}$, and inverse EST of $\mathbf{y}$ is $\mathcal{E}^{-1}(\mathbf{y}) = \mathbf{E}^H\mathbf{y}$. Ideal EST can equally spread the energy of symbol vector, $\mathbf{x}$, to whole time and frequency band. Ideal EST satisfy the two following energy spreading conditions.

- Time Energy Spreading Condition:

$$\sum_{l=0}^{N-1}(|(\mathbf{E^H})_{l,n}|^2 - \frac{1}{N})^2 \approx 0 \tag{24}$$

- Frequency Energy Spreading Condition:

$$\sum_{l=0}^{N-1}(|(\mathbf{FE})_{l,n}|^2 - \frac{1}{N})^2 \approx 0 \tag{25}$$

Ideal EST is a set of basis and each of its basis are equally projected to Fourier basis or $\mathbf{e}_i$ whose i th element is 1 and rest of them are zeros. In order to equally spread

the error energy induced from the time domain, each basis of $\mathbf{E}$ should be equally projected to the time domain basis $\mathbf{e}_i$. Similarly, $\mathbf{E}$ also have to be equally projected on the Fourier basis.

Intuitively, the relations between Identity, Fourier and EST matrices can be simplified as figure 7. In figure 7, $\overrightarrow{\delta}_i$, $\overrightarrow{e}_i$, and $\overrightarrow{f}_i$ are the i th colum vector of Identity, EST and DFT matrices. Arrow to $|\cdot| = \overrightarrow{1}$ means that vector at the starting point is transformed into a flat amplitude vector.

However finding Ideal EST is difficult and there are no closed formulation or method to derive Ideal EST. So Hwang proposed a way to construct an empirical EST.

$$\mathbf{E} = \prod_{i=0}^{m} \mathbf{P^{(i)}} \mathbf{M} \tag{26}$$

where $\mathbf{P^{(i)}}$ is a random permutation matrix and $\mathbf{M}$ is an orthonormal matrix with N Frobenius norm such as normalized Hadamard matrix or discrete-Fourier matrix. Therefore, both EST and Inverse EST (IEST) require $O\big(mNlog(N)\big)$ complex multiplications.

4.2.2 EST based IDFE

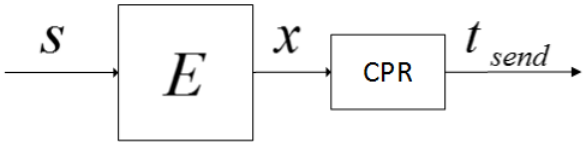

Figure 8: EST based IDFE Transmitter

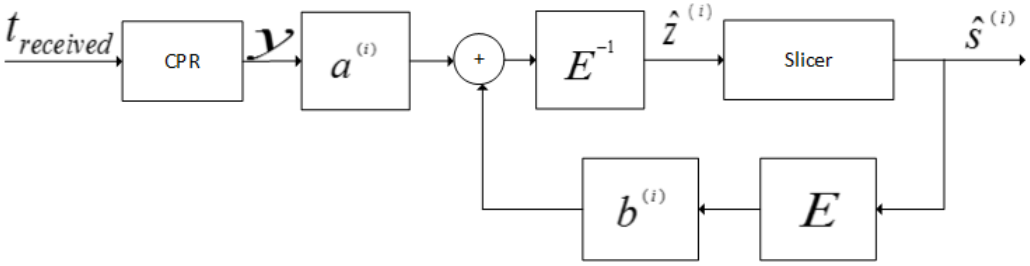

Figure 9: EST based IDFE Receiver

In [15], he suggested Energy Spreading Transform (EST) as an add-on method for Iterative Decision Feed back Equalization (IDFE). EST makes IDFE more robust to localized errors in frame. By combining the IDFE with EST, Hwang designed an EST based IDFE in [15] and it converges to the matched filter bound asymptotically.

For instances, let us assume the detected symbols in i step iterations are $\hat{\mathbf{s}}^{(i)}$ and for simple notation, the channel length of $\mathbf{c}$ is 5. Since gain of c_j in multipath channel or FTNS are generally skewed or localized in some j, we also assume that $|c_0| > |c_{\pm 1}| > |c_{\pm 2}|$. Now Suppose $\hat{\mathbf{s}}^{(i)}$ has localized errors from $\hat{s}_{n-2}^{(i)}$ to $\hat{s}_{n+2}^{(i)}$ and all the other symbols are correctly detected. So SER is $\frac{5}{N}$ in (i) steps. Then $\hat{s}_{n-2}^{(i+1)}$ to $\hat{s}_{n+2}^{(i+1)}$ are computed from the below equations.

$$
\begin{aligned}
y_{n-2} &= c_{-2}\cdot \hat{s}_{n-4}^{(i)} + c_{-1}\cdot \hat{s}_{n-3}^{(i)} + c_0 \cdot s_{n-2}^{(i+1)} + \underbrace{c_1 \cdot \hat{s}_{n-1}^{(i)} + c_2 \cdot \hat{s}_{n}^{(i)}}_{\text{Error}} + \underbrace{w_{n-2}}_{\text{Noise}} \\
&\vdots \\
y_{n} &= \underbrace{c_{-2}\cdot \hat{s}_{n-2}^{(i)} + c_{-1}\cdot \hat{s}_{n-1}^{(i)}}_{\text{Error}} + c_0 \cdot s_{n}^{(i+1)} + \underbrace{c_1 \cdot \hat{s}_{n+1}^{(i)} + c_2 \cdot \hat{s}_{n+2}^{(i)}}_{\text{Error}} + \underbrace{w_{n}}_{\text{Noise}} \\
&\vdots \\
y_{n+2} &= \underbrace{c_{-2}\cdot \hat{s}_{n}^{(i)} + c_{-1}\cdot \hat{s}_{n+1}^{(i)}}_{\text{Error}} + c_0 \cdot s_{n+2}^{(i+1)} + c_1 \cdot \hat{s}_{n+1}^{(i)} + c_2 \cdot \hat{s}_{n+3}^{(i)} + \underbrace{w_{n+4}}_{\text{Noise}}
\end{aligned}
\tag{27}
$$

In equation 27, although the overall SER is very small when N is large, it is difficult for IDFE to detect the symbols from $\hat{s}_{n-2}^{(i+1)}$ to $\hat{s}_{n+2}^{(i+1)}$ correctly. Because the neighboring symbols decided in previous step, $\hat{s}_{n-2:n+2}^{(i+1)}$, were incorrect and power gain factor of those neighboring terms, $\mathbf{c}_j$, are localized. Thus IDFE itself is not robust to this type of localized errors.

However, If EST is applied, y_n is not a function of the neighboring symbols around s_n but a function of whole symbols in the frame.

$$
y_n = g_0 \cdot \hat{s}_1^{(i)} + \cdots + + g_n \cdot \hat{s}_n^{(i+1)} + \cdots + g_{N-1} \cdot \hat{s}_{N-1}^{(i)} + w_n \tag{28}
$$

Also since $|g_i| \approx |g_j|$, each $\hat{s}_m^{(i)}$ equally affect $\hat{s}_n^{(i+1)}$ regardless of n and m. Thus $\hat{s}_n^{(i+1)}$,

in equation 28, converges to s_n as long as N is large and SER is larger than 0.5.

To specify, Incorrectly determined symbol in IDFE, $\hat{x}_n^{(i)} \neq x_n$, locally affect the next decision step $\hat{x}_n^{(i+1)}$. Error energy, $e_n^{(i)} = \hat{x}_n^{(i)} \neq x_n$, is also locally spread across the neighboring symbols, $\hat{x}_{n\pm m}^{(i+1)}$. Thus, next decision of the symbols around n tends to be incorrect if $\hat{x}^{(i)}[n]$ is incorrect. But energy spreading transform (EST) can spread this error energy of previous iteration to whole block in both time / frequency band, so incorrectly detected symbols in previous step equally affect the next iteration symbol decision and next iteration does not suffer burst of error energies.

4.2.3 IDFE with frequency-interleaved encoding

One thing we should note is that the similarity between EST based IDFE and IDFE with frequency-interleaved encoding [8]. As we mentioned in sec:4.1, the transmitter-receiver scheme of FD-IDFEs are similar to each other. In [8], the proposed transmitter send the signal by randomly interleaving its frequency response coefficients, sending $\mathbf{x} = \mathbf{FPF^H s}$ instead of $\mathbf{s}$. But it can be also described as a special case of EST based IDFE when $\mathbf{E} = \mathbf{F^H PFs}$.

Thus, our proposed FTNS scheme in this thesis can be regarded as an application of both extension of the frequency-interleaved encoding and the energy spreading transform.

4.3 Summary

We reviewed IDFE first and explained the idea of EST and how EST improve the performance of IDFE.

CHAPTER V

ANALYSIS ON EST BASED IDFE

In Chapter 5, we investigated the some issues of EST based IDFE and couple of them have not been researched yet in other papers. Firstly, we suggested several ways to enhance the performance of EST based IDFE equalizer with a brief summary of IDFE structure. Secondly, we will see a way to construct Ideal EST matrix and compare its performance to normal EST. And we explain a mathematical properties of EST which can be an alternative explanation of why EST can enhance other IDFE performance.

5.1 Applying EST to IDFE

As a reminder, EST is an add-on method for IDFE. Thus, depending on what kind of IDFE we choose, the equalizer performance changes. In this section I applied EST to other IDFEs and suggest a simple way to enhance IDFE performance.

Let us generalize IDFE structure. There are many researches on IDFE and each of them has its own FF and FB filters update criterion. But when it comes to implementation, they all have the same structures as equation 29 and 30.. Also the intermediate derivation of each IDFE algorithms are overlapping each others.

Let us assume the receive signal $\mathbf{y}$ is described in a discrete time channel model $\mathbf{y} = \mathbf{c} * \mathbf{s} + \mathbf{w}$ and the block size is N.

$$\text{FF filter:} \quad A_k^{(i+1)} = \frac{\gamma_n^{(i+1)} C_k^*}{\gamma_d^{(i+1)} |C_k|^2 + \sigma_w^2} \tag{29}$$

$$\text{FB filter:} \quad B_k^{(i+1)} = A_k^{(i+1)} C_k - \mathbb{E}[A_k^{(i+1)} C_k] \tag{30}$$

$$\gamma_d^{(i)} = 1 - \mathbb{E}^2[s\hat{s}], \qquad \gamma_n^{(i)} = \text{Normalization factor} \tag{31}$$

Where $\{C_k\}$, $\{A_k^{(i)}\}$, and $\{B_k^{(i)}\}$ are FFTs of $\mathbf{c}$, $\mathbf{a}^{(i)}$ and $\mathbf{b}^{(i)}$ and σ_w^2 is the noise power. I also noted the average value of $A_k^{(i)} C_k$ along the frequency bin k as $\mathbb{E}[A_k^{(i)} C_k]$. Since

$\gamma_n^{(i)}$ is a normalization factor, the result of 29 and 30 depend on the values of $\gamma_d^{(i)}$. This parameters,$\gamma_d^{(i)}$, is an estimates of $1 - \mathbb{E}[s\hat{s}]^2$

5.1.1 Selection of Feed-forward Filter

Most of FD-IDFE demodulation algorithms can be described in the form of equation (29) and (30). And $\gamma_d^{(i)}$ and $\gamma_n^{(i)}$ are the only differences between them. The internal IDFE algorithm that Hwang had proposed with EST in [17] can also be expressed in this form as

1. Hwang: the IDFE proposed with EST [16]

   $\mathbf{g}^{(i)} = \mathcal{F}^{-1}(A_k^{(i)} C_k), \qquad K_h^{(i)} = \sum_{n \neq 0} |g_n^{(i)}|^2 / |g_0^{(i)}|^2$

   $P_{no}^{(i)} = \frac{\sigma_w^2}{N} \parallel \mathbf{a^{(i)}} \parallel^2, \qquad P_{isi}^{(i)} = (\gamma_d^{(i)})^2 K_h^{(i)}$

   $\widehat{\mathrm{SINR}}_{in}^{(i)} = \frac{1}{P_{isi}^{(i)} + P_{no}^{(i)}}, \qquad \widehat{\mathrm{SER}}^{(i)} = 1 - \left(1 - 2\left(1 - \frac{1}{\sqrt{M}}\right)\mathcal{Q}\left(\sqrt{\frac{3\mu^i}{M-1}}\right)\right)^2$

   $\gamma_d^{(i+1)} = \kappa(\widehat{\mathrm{SER}}^{(i)})\widehat{\mathrm{SER}}^{(i)} = \frac{4\widehat{\mathrm{SER}}^{(i)}}{(2 - 0.5\widehat{\mathrm{SER}}^{(i)})}$, when $M = 4$.

The approximated functional relation, $\kappa(\cdot)$, between expected symbol error value and given SER is depend on signal constellation and gray code.

Similarly We can also rewrite other 4 different IDFE methods [5, 7, 25, 26] in this form. Of course there are minor differences between them, such as the type of cyclic extension, block size or iteration size. But they all share the common structure. Here are the summary of 4 different hard-decision IDFE equalizers which update $\gamma_d^{(i)}$ and $\gamma_n^{(i)}$ differently. For simple notation, we assume that the signal powers of both estimated signal $\hat{s}$ and actual signal s are equal to one.

2. Chan [7]

   $\alpha_k^i = \frac{1}{\sigma_w^2} \cdot (1 - (\rho_s^{i-1})^2) \cdot |A_k|^2$

   $\widehat{\mathrm{SINR}}_{in}^{(i)} = \left(\frac{1}{\mathbb{E}_k\left[\frac{1}{1+\alpha_k^i}\right]} - 1\right) \cdot \frac{1}{1 - (\rho_s^{i-1})^2}, \qquad \widehat{\mathrm{SER}}^{(i)} = 1 - \left(1 - 2\left(1 - \frac{1}{\sqrt{M}}\right)\mathcal{Q}\left(\sqrt{\frac{3\mu^i}{M-1}}\right)\right)^2$

   $\rho_s^i = 1 - 2sin^2(\frac{\pi}{M})\widehat{\mathrm{SER}}^{(i)}$

   $\gamma_d^{(i+1)} = (1 - (\rho_s^i)^2)$

3. Sainte (1) [25]

   $\gamma_n^{(i)} = 1 - \frac{i}{K}$, K is the maximum iteration number

   FF filter: $A_k^{(i+1)} = \frac{\gamma_n^{(i+1)} C_k^*}{|C_k|^2 + \sigma_w^2} + (1 - \gamma_n^{(i+1)}) C_k^*$

The $\gamma_d^{(i)}$ and $\gamma_n^{(i)}$ of the first three methods depend on the iteration step i, channel response $\mathbf{a}$ and SNR, but do not depend on the determined value $\hat{\mathbf{s}}$ and the received signal $\mathbf{y}$. Otherwise the rest two use the estimates of SINR and SER as intermediate parameters to calculate $\gamma_d^{(i)}$ and $\gamma_n^{(i)}$.

4. Sainte (2) [26]

   $l = 2\sigma_u^2 + 4\int_1^\infty u f(u) du$, where $\mathbf{u} = \hat{\mathbf{z}}^{(i-1)} - \mathbf{s}$, and $f(\cdot) = \mathcal{N}(0, \sigma_u^2)$.

   $e = \hat{\mathbf{z}}^{(i-1)} - \hat{\mathbf{s}}$

   $\gamma_d^{(i)}, \gamma_n^{(i)} = \sigma_e^2 + l$

5. Benvenuto [5]

   $0 < \mu < 1$

   $\rho_s^i = (1 - \mu) \sum \frac{Y_k}{C_k} \hat{S}_k^{(i)*}$

   $\gamma_d^{(i+1)} = (1 - (\rho_s^i)^2)$

One big difference between Sainte (2) [26] and others is that [26] use the pre-computed (simulated) statistical information of exact error, $\mathbf{u} = \hat{\mathbf{z}}^{(i-1)} - \mathbf{s}$. It also assumes that $\mathbf{u}$ follows complex Gaussian distribution.

All these five algorithms are derived based on the assumption that $\hat{s}$ and $s - \hat{s}$ are statistically independent. As Hwang combined EST to IDFE in [16], we applied EST to the rest of IDFEs. We tested both IDFEs and IDFEs with EST in frequency selective channels and analyze how EST change other IDFE performances.

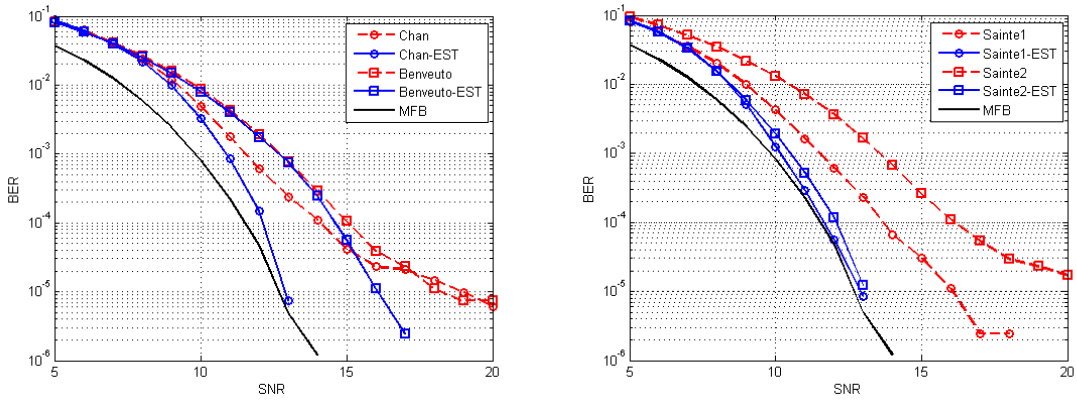

(a) Chan, Benvenuto (b) Sinte (1), Sainte (2)

Figure 10: $\mathbf{h} = [.485 - i.097 \quad .364 + i.437 \quad .243 \quad .291 - i.315 \quad .194 + i.388]$

The simulation result shows that all the other IDFE's performances in a frequency selective channel are enhanced by EST as in figure 10. However if the channel is not frequency selective or does not have null-frequency region, the performance gap between with and without EST is very small. Therefore, we can conclude that EST enhance the robustness of class of iterative equalizers regardless of their internal filter update criteria.

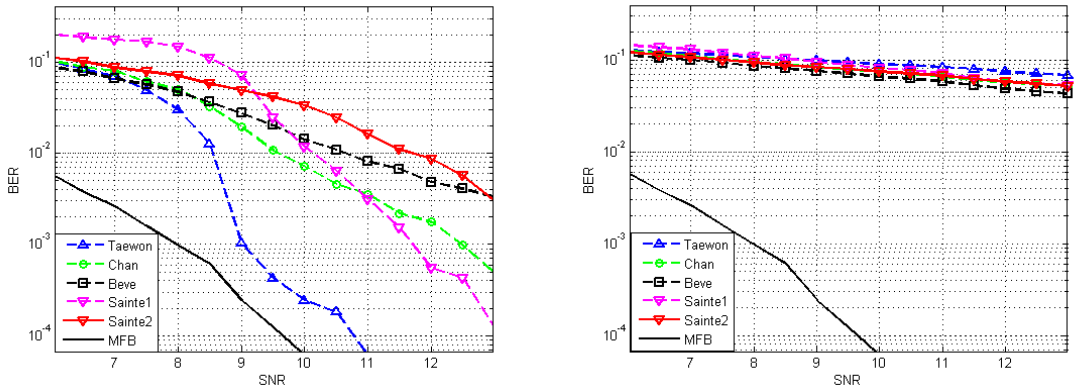

(a) IDFEs with EST (b) IDFEs without EST

Figure 11: $\rho = 0.8$, $\beta = 0.3$, $\psi(t) \neq 0$ when $t \in [-40\rho T, 40\rho T]$ and $\mathbf{h} = [.407.815.407]$

But still Hwang's IDFE shows the best performance when it is combined with EST. Both figure (11a) and (11b) are simulated in the same channel condition, a frequency selective channel under FTNS. The simulation result showed that the performance of original Hwang's IDFE and EST pairs is better than other EST and IDFE pairs.

As we can see IDFEs themselves are not robust to null frequency channel spectrum induced by physical channel vector $\mathbf{c}$.

5.1.2 Infrequent filter update

In Hwang's IDFE, the algorithm .1, $\gamma_d^{(i)}$ and $\gamma_n^{(i)}$ are functions of estimated SER, $\widehat{\mathrm{SER}}(\tilde{\mathbf{z}}^{(\mathbf{i})})$, which is an another function of estimated SINR, $\widehat{\mathrm{SINR}}(\tilde{\mathbf{z}}^{(\mathbf{i})})$. Thus, $\widehat{\mathrm{SINR}}(\tilde{\mathbf{z}}^{(\mathbf{i})})$ determines the performance of equalizer.

The simulation result showed that actual SINR is different to the estimated SINR unless the channel is a flat fading channel, $\mathbf{c} = \delta[n]$. Also even if $\widehat{\mathrm{SINR}}^{(i)}$ is replaced into the actual $\mathrm{SINR}^{(i)}$, as the algorithm 4. [26], the equalizer's performance does not change much.

But, one interesting thing we had observed is that if we stop updating the filter ,$\mathbf{a}^{(\mathbf{i})}$ and $\mathbf{b}^{(\mathbf{i})}$, after i step and keep iterating the decision process, the actual SINR converge to the higher value when i is small.

Motivated by this result, we updated $\mathbf{a}^{(\mathbf{i})}$ and $\mathbf{b}^{(\mathbf{i})}$ once in a few step in instead of every iteration step as [16]. When filter updates are skipped, each iteration requires only $N + 2NlogN + 2\mathcal{O}_{EST}(NlogN)$ complex multiplication. With filter updates, each iteration needs additional $4N + 2NlogN$ complex multiplications. Since we used the simplest EST ($\mathbf{E} = \mathbf{FP}$) for the simulation in this subsection $\mathcal{O}_{EST}(NlogN)$ is $\mathcal{O}_{EST}(NlogN) = NlogN$.

In Figure (12), two different EST based FTNS schemes, EST1 and EST2, are compared in a frequency selective channel, Proakis-c channel. The 1st iteration steps of both equalizers are same. But under EST1, filter coefficients are updated in every iteration [16], while under EST2, filter coefficients are updated once in every two iterations.

Both EST1 and EST2 are converged around the 7 iteration steps. But EST2 converges in lower SNR than EST1. Also the computational power required for EST1

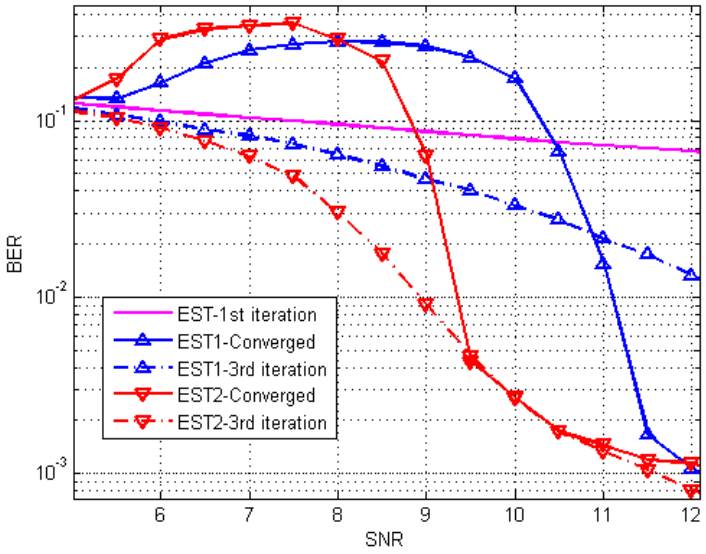

Figure 12: BER versus SNR for an EST based FTNS system with $\rho = 0.7$, $\beta = 0.3$, $\psi(t) \neq 0$ when $t \in [-30\rho T, 30\rho T]$ and $\mathbf{h} = [.485 - i.097 \quad .364 + i.437 \quad .243 \quad .291 - i.315 \quad .194 + i.388]$

to do 7 iterations, $42NlogN + 35N$, is almost the same as that required for EST2 to iterate 3 steps, $42NlogN + 21N$. 3rd iteration result of EST2 is better than all the results of EST1. Although the both physical channel condition and FTNS condition are severe, BER of EST2 approaches to MFB at lower SNR than BER of EST1 does.

One thing to note is that the algorithm used in this simulation is slightly different to the original one in [16] due to the constraints of FTNS. We will see the differences in next chapter.

5.1.3 Soft-decision demodulation

One thing we should note here is that we do not consider soft-decision IDFE equalizers which calculate the two parameters, $\gamma_n^{(i+1)}$ and $\gamma_d^{(i+1)}$, by using Log-Likelihood of $hats^i$. If we also consider soft-decision demodulation equalizers, there are far more candidates and we should consider error-correcting coding performance. Because soft-decision method can be simply extended to Turbo Equalization which is an another huge topics. So we only consider γ_d estimation method grounded on hard-decision

demodulation

5.2 Analysis on EST

Until now only a few EST researches have been conducted in application perspective. Furthermore, although these conditions of EST were proposed in 2006, no one has suggested an ideal EST which satisfy the conditions yet. Therefore, we firstly propose one way to construct Ideal EST matrix and explain one problem in previous researches on EST. Secondly we will see the mathematical property of non-ideal EST and suggest alternative explanations on the reason why EST enhance IDFE performance.

5.2.1 Ideal EST

The EST which Hwang had proposed in the first EST paper does not exactly satisfies the spreading conditions (LHS of equation 30). He also insisted that these spreading conditions determines the performance of equalizer. His EST, $\mathbf{E} = \prod_{i=0}^{m} \mathbf{P^{(i)}M}$, satisfies the conditions asymptotically when the matrix size N is large and its norm is fixed.

$$\begin{aligned} \sum_{l=0}^{N-1}(|(\mathbf{E^H})_{l,n}|^2 - \frac{1}{N})^2 = 0 \\ \sum_{l=0}^{N-1}(|(\mathbf{FE})_{l,n}|^2 - \frac{1}{N})^2 = 0 \end{aligned} \tag{32}$$

Finding ideal EST directly from the equation 32 is intractable for $N > 2$. But with the prior knowledge from the second equation of 32 that each basis (column vector) of EST should be a sum of DFT basis and the amplitude of its DFT coefficients should be equal to $1/\sqrt{N}$, we can reduce the number of unknowns in $\mathbf{E}$ from N^2 to N.

To specify, if we find a coefficient vector $\mathbf{c}$ such that $c_i \neq c_j$ and $|c_i| = 1/\sqrt{N}$, we can construct N independent vectors by multiplying circularly shifted $\mathbf{c}$ with DFT matrix $\mathbf{F}$. Matrix $\mathbf{E}$ obtained from the below process satisfies equation 30 without any residual.

Listing 5.1: Constructing Ideal EST matrix when N is a even number

```
F = dftmtx(N)/sqrt(N);
p = 1:1:N;   p = aix.^2;   p=exp(2i*pi*aix/(2*N));
E = gallery('circul',p );
```

Since $\mathbf{E}$ is a circulant matrix of vector $\mathbf{p}$, $\mathbf{Ex} = \mathbf{p} \circledast \mathbf{x}$ needs only $2NlogN+N$ complex multiplication.

The other important aspect of EST is that EST is not unique. We confirmed that there are infinite number of non-parallel basis sets which satisfy the EST condition (equation 30) in when N is small ($N < 8$). Especially when $N = 2$ $\mathbf{E}$ has two degree of freedom so there are infinite number of $\mathbf{E}$ for given N.

Next, we compare the performance of gap between EST based IDFE and Ideal EST based IDFE. We noted EST_{aprx} and $\text{EST}_{\text{ideal}}$ for non-ideal and ideal EST.

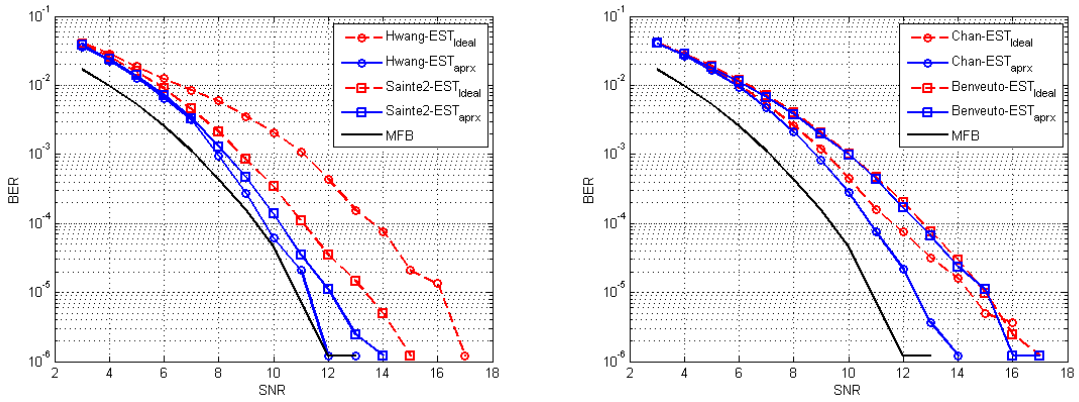

(a) Hwang and Sainte (b) Chan and Benvenuto

Figure 13: Comparison between EST based IDFE and Ideal EST based IDFE

Surprisingly, the IDFE with ideal EST shows worse performance than IDFE with non-ideal EST, repeated Fourier and Permutation matrix, for all cases. This simulation result implies that the spreading condition is not a good measure of performance and the higher performance of non-ideal EST should be explained in other way which may not be related with spreading conditions.

5.2.2 EST as a Random Projection

In [15], the derivation of FF filer and FB filter in IDFE is related with the energy spreading properties of EST. But in previous subsection, we observed that the energy spreading conditions are not good way to explain the better performance of EST. Therefore alternative explanation is required to explain the better performance of non-ideal EST over ideal-EST.

According to [17], the decision error energy term, diagonal elements of $\mathbf{ER_dE}$, approach to Gaussian random vector by central limit theorem when $\mathbf{E}$ is a Ideal EST whose L2 norm of each element is $1/\sqrt{N}$. Where $\mathbf{R_d}$ is covariance matrix of decision error of $\hat{\mathbf{z}}$. R_d is the covariance matrix of decision error of $\hat{\mathbf{z}}$.

But Gaussian property of $\mathbf{E}\bar{\mathcal{D}}(\cdot)\mathbf{E}$), which is the interference power, can also be explained with the empirical EST and without introducing Ideal EST (we used $\bar{\mathcal{D}}(\cdot)$ to note off-diagonal elements of matrix).

Let us see how the empirical EST changes as i increases. Simulation result shows that the empirical EST matrix itself becomes a sampled Gaussian matrix when both m and N are large ($N > 2^{10}$ and $m > 2$).

$$\begin{aligned} \mathbf{E} &= \prod_{i=0}^{m} \mathbf{P^{(i)}M} \\ &\approx \{e_{ij}\}, \qquad e_{ij} \sim \mathcal{N}(0, 1/N) \end{aligned} \tag{33}$$

where e_{ij} is a complex Gaussian random variable. Thus we can threat EST as an random projection operator. Therefore $\mathbf{Es}$ also becomes a Gaussian vector due to the central limit theorem. To visualize this effect, we chose $\mathbf{M} = \mathbf{H}$, where $\mathbf{H}$ is Hadamard matrix and draw the distribution of the elements $\mathbf{E}$ depending on m.

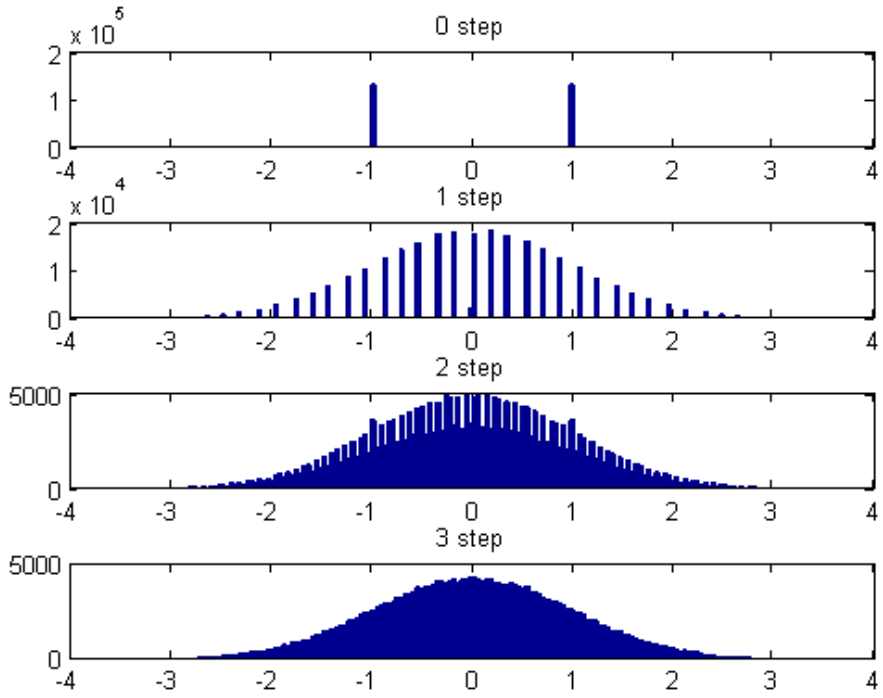

Figure 14: Histograms of matrix elements in the repeated Hadamard and Permutation matrices: $\mathbf{H}$, $\mathbf{HP}_1\mathbf{H}$, $\mathbf{HP}_2\mathbf{HP}_1\mathbf{H}$, $\mathbf{HP}_3\mathbf{HP}_2\mathbf{HP}_1\mathbf{H}$

Figure 14 shows that how the distribution of repeated Hadamard and Permutation matrices converges to a Gaussian distribution. As we keep multiplying normalized Hadamard and Permutation matrix to itself, the distribution of its elements approaches a sampled random Gaussian distribution, $e_{ij} \sim N(0, 1/N)$ whose variance is equal to 1. Also if the matrix size N is large, It approaches to a Gaussian distribution much faster.

And if we assume that EST is a Gaussian random projection operator, we can more easily understand the justification of EST mentioned in the previous section 4.2.2. Let us see the equation 28 one more time.

$$y_n = g_0 \cdot \hat{s}_1^{(i)} + \cdots + + g_n \cdot \hat{s}_n^{(i+1)} + \cdots + g_{N-1} \cdot \hat{s}_{N-1}^{(i)} + w_n \tag{34}$$

If we assume EST is a sampled Gaussian matrix, the value of $\mathbf{g}$ become a complex

Gaussian value due to the Central limit theorem. Then we can describe 34 as

$$\begin{aligned} y_n - \mathbf{g}^* \cdot \mathbf{s}^{(i)} + w_n &= \mathbf{g}^* \cdot (\mathbf{s} - \hat{\mathbf{s}}^{(i)}) \\ &\approx \mu \cdot \sigma_s \cdot N_d \end{aligned} \tag{35}$$

where N_d is the number of error symbol, μ is a unit Gaussian noise and σ_s is the square root of the signal power. Therefore all y_n have the similar interference noise statistics which is a Gaussian distribution.

If the interference term follows Gaussian distribution, symbol-by-symbol decision method, what slicer does, is the ideal way to decide a symbol vector $\mathbf{s}$ from $\hat{\mathbf{z}}^{(\mathbf{i})}$. To specify, the explicit equation of i step input of the slicer is described as

$$\begin{aligned} \hat{\mathbf{z}}^{(\mathbf{i})} &= \mathbf{A}^{(\mathbf{i})}\mathbf{y} + \mathbf{B}^{(\mathbf{i})}\mathbf{E}\hat{\mathbf{s}}^{(i-1)} \\ &= \mathbf{E}^{\mathbf{H}}\mathbf{A}^{(\mathbf{i})}\mathbf{C}\mathbf{E}\mathbf{s} + \mathbf{E}^{\mathbf{H}}\mathbf{B}^{(\mathbf{i})}\mathbf{E}\hat{\mathbf{s}}^{(i-1)} + \mathbf{E}^{\mathbf{H}}\mathbf{A}^{(\mathbf{i})}\mathbf{w} \\ &= \underbrace{\mathbf{I}\mathbf{s}}_{\text{Signal}} + \underbrace{\mathbf{E}^{\mathbf{H}}\bar{\mathcal{D}}(\mathbf{A}^{(\mathbf{i})}\mathbf{C})\mathbf{E}(\hat{\mathbf{s}}^{(i-1)} - \mathbf{s})}_{\text{Interference}} + \underbrace{\mathbf{A}^{(\mathbf{i})}\mathbf{w}}_{\text{Noise}} \\ &= \mathbf{s} + \nu + \tilde{\mathbf{w}}, \qquad \nu \sim \mathcal{N}(0, \sigma_d) \end{aligned} \tag{36}$$

Now all noise components v and $\tilde{\mathbf{w}}$ are statistically independent from the perspective of symbol block vector ν. Therefore deciding s_n one by one is the best symbol decision method.

Our approach does not introduce the concept of spreading properties. Moreover, the more elements of $\mathbf{E}$ shows Gaussian distribution property, the more interference term $\mathbf{E}^{\mathbf{H}}\bar{\mathcal{D}}(\mathbf{A}^{(\mathbf{i})}\mathbf{C})\mathbf{E}(\hat{\mathbf{s}}^{(i-1)} - \mathbf{s})$ follows Gaussian distribution. Therefore, it also can explain the better performance of non-ideal EST over ideal-EST.

Furthermore, this explanation can also be applied to all different types of IDFEs we saw in previous sections.

5.3 Summary

In this chapter, we have investigated the possible variations of EST based IDFE. Hwang's IDFE showed better performance than other IDFEs when they are combined

with EST and its performance is further enhanced by updating filter infrequently. Moreover we suggested both Ideal EST and the alternative explanation of non-Ideal EST to explain the contradiction that Ideal EST show worse performance than non-Ideal EST.

CHAPTER VI

APPLYING EST BASED IDFE TO FTNS

Chapter 6 elaborates FTNS performance of EST based IDFE. At first, we will look at the discrete time channel model we used to describe FTNS Secondly, EST based IDFE for that channel model is summarized. Then, The pseudo code of FTNS scheme we tested is summarized. Finally we analyses how our equalizer handles the difficulties of using FDE for FTNS including those we explained in chapter 3.

6.1 FTNS as a Channel with Colored Gaussian Noise

In this section, we will explain an another discrete channel model we used in the following chapters to describe FTNS. By using this model, FTNS can be expressed as a colored noise frequency selective channel signaling. Therefore, It allows us utilize many of the frequency selective channel demodulation methods, including EST based IDFE, to FTNS problem.

6.1.1 Proposed Discrete Time Channel Model

The discrete channel model we will see in this section is an intermediate model between Ungerbeock model and WMF model. Unlike WMF model, only the actual channel $\mathbf{h}^{-*}$ components are whitened from the noise vector $\mu = \mathbf{h}^{-*} * \psi^{-*} * \mathbf{w}$. This is the same filter in Nyquist signaling but it can not whiten the noise in FTNS. Let the minimum phase component of $\mathbf{h} * \mathbf{h}^{-*}$ is $\mathbf{h}_{min}$, then the model used in next sections is described as equation (37).

$$\mathbf{y} = \mathbf{c} * \mathbf{s} + \mathbf{w} \tag{37}$$

$$\mathbf{c} = \mathbf{h}_{min} * \mathbf{r}_{\psi\psi} \tag{38}$$

$$\mathbf{w} = \boldsymbol{\psi}^{-*} * \boldsymbol{\nu}, \quad \boldsymbol{\nu} \sim \boldsymbol{\mathcal{N}}(\mathbf{0}, \boldsymbol{\sigma}_{\boldsymbol{\nu}}^{\mathbf{2}}) \tag{39}$$

Then we applied EST based FTNS to the equation (37).

6.1.2 Noise Spectrum

In this model, noise vector **w** is not white. Thus the noise spectrum, W_k, should be considered. $W_k = \sigma_w \cdot \Psi_k$ where σ_w and Ψ_k are noise variance and the DFT coefficients of sampled modulation pulse ψ. Therefore, Feed-Forward filter **a** turns into the equation (40) in frequency domain.

$$\text{Feed-Forward filter:} \quad A_k^{(i+1)} = \frac{\gamma_n^{(i+1)} C_k^*}{\gamma_d^{(i+1)} \parallel C_k \parallel^2 + \parallel W_k \parallel^2} \tag{40}$$

The noise spectrum of **w** is same as ρT sampled modulation pulse $\psi(t)$. As Figure 5 showed, $\mathbf{r}_{\psi\psi}$ is frequency selective and its frequency selectivity is determined by ρ and β. As a reminder, ρ is the 3dB cut-off frequency, β is a transition region factor and the length of $\psi(t)$ determines the number of null frequency component $\mathbf{r}_{\psi\psi}$.

To sum up, we can treat SC-FTNS, equation 37, as SC NS through an frequency selective channel with colored Gaussian noise.

6.2 Proposed FTNS Scheme

Based on the simulation result of chapter 5, we propose an EST based IDFE modulation and demodulation scheme for FTNS in this section. Non-ideal EST and infrequently updated IDFE are applied to the discrete time channel model of FTNS we saw in previous section. We also briefly explain two other FDE based FTNS schemes we used in simulations to compare the performance of my proposed equalizer.

6.2.1 EST based IDFE for FTNS

Unlike normal SC-FDE and OFDM, Inserted CP length is far less than the channel vector length **c**. This issues will be discussed in the next section.

Algorithm 1 Modulation:

$\mathbf{s}$ = QPSK symbol sequence
procedure MODULATION
    $\mathbf{x} = \mathbf{Es}$
    $\mathbf{t_{send}}$ = Insert_CP($\mathbf{x}$)
    Transmit $\mathbf{t}_{send}$ via Linear pulse modulator.
end procedure

Algorithm 2 Demodulation:

Ensure: $\mathcal{F}(\cdot)$ is fast Fourier transform, $\mathcal{E}(\cdot)$ is energy spreading transform.
$Y_k = \mathcal{F}(\mathbf{y})$, $C_k = \mathcal{F}(\mathbf{c})$, $A_k^{(i)} = \mathcal{F}(\mathbf{a}^{(i)})$, $B_k^{(i)} = \mathcal{F}(\mathbf{b}^{(i)})$
$A_k^{(0)}$ = Minimum mean square error equalizer
$p_{sig} = 1$, $\gamma_d^{(0)} = 1$
Channel coefficients $\mathbf{c}$ is know to receiver.
procedure DEMODULATION
    $\mathbf{y}$ =Remove_CP($\mathbf{t}_{receive}$)
    for $i := 1$ to 5, step 1 **do**
        $\mathbf{g}^{(i)} = \mathcal{F}^{-1}(A_k^{(i)} C_k)$
        $B_k^{(i)} = A_k^{(i)} C_k - E[A_k^{(i)} C_k]$
        for $j := 1$ to 3, step 1 **do**
            $\mathbf{z}^{(i)} = \mathcal{E}^{-1}(\mathcal{F}^{-1}(A_k^{(i)} Y_k - B_k^{(i)} \mathcal{F}(\mathcal{E}(\hat{\mathbf{s}}))))$
            $\hat{\mathbf{s}} :=$ Slicer($\mathbf{z}^{(i)}$)
        end for
        $K_h^{(i)} = \sum_{n \neq 0} |g_n^{(i)}|^2 / |g_0^{(i)}|^2$
        $P_{no}^{(i)} = \frac{\sigma_w^2}{N} \parallel \mathbf{a^{(i)}} \parallel^2$
        $P_{isi}^{(i)} = (\gamma_d^{(i)})^2 K_h^{(i)}$
        $\widehat{\mathrm{SINR}}_{in}^{(i)} = \frac{P_{sig}}{P_{isi}^{(i)} + P_{no}^{(i)}}$
        $\widehat{\mathrm{SER}}^{(i)} = \frac{1}{2}(1 - erf(\sqrt{\widehat{\mathrm{SINR}}_{in}^{(i)}}))$
        $\gamma_d^{(i+1)} = \kappa(\widehat{\mathrm{SER}}^{(i)}) \widehat{\mathrm{SER}}^{(i)} = \frac{4\widehat{\mathrm{SER}}^{(i)}}{(2 - 0.5\widehat{\mathrm{SER}}^{(i)})}$
        $\gamma_n^{(i+1)} = (\frac{1}{N} \Sigma_k \frac{|C_k|^2}{(\gamma_d^{(i+1)})^2 |C_k|^2 + \sigma_w^2})^{-1}$
        $A_k^{(i+1)} = \frac{\gamma_n^{(i+1)} C_k^*}{(\gamma_d^{(i+1)})^2 |C_k|^2 + |W_k|^2}$
    end for
end procedure

6.2.2 Comparison

We compared the performance of our EST based IDFE FTNS scheme to other two FDE based FTNS schemes: MMSE [28] and fractionally over-sampled Iterative Block

Decision feedback equalizer (IBDFE) [29]. Equalizer in [29] is an another variation of IDFE. In [29] FTNS scheme, receiver samples the output of matched filter two times more than IDFE thus its internal FF and FB filtering size is $2N$.

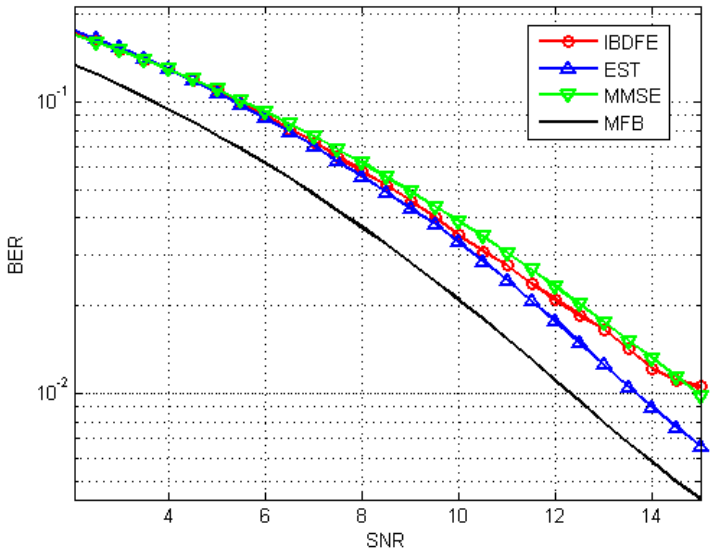

Figure 15: BER of the FDE based FTNS schemes in $\rho = 0.8$, $\beta = 0.3$, $\psi(t) \neq 0$ when $t \in [-40\rho T, 40\rho T]$ and $\mathbf{h}$ is a exponentially decaying Raleigh fading channel and the length of CP is 16

In figure 15, symbol transmission rate is 25% higher than Nyquist signaling and our equalizer converges to MFB bound. The performance of equalizers varies as the FTNS parameter: ρ, β and CP length, change. As we discussed in section 3.4, if these parameters are too large or small, FDE performance decreases. We will see the simulation result in these situations in the next section.

6.3 Problems of applying FDE based FTNS

In section 3.4, we checked couple of difficulties of using FDE for FTNS. This section will demonstrate the robustness of our proposed equalizer to those difficulties. The first difficulty is that the channel estimation error entailed by insufficient Cyclic Prefix. It came from the long channel memory of $\mathbf{c}$. Then, we will see how the proposed equalizer behave under the colored noise. Performance analysis under the

regularization is also discussed.

6.3.1 Channel Estimation Error: Insufficient Cyclic Prefix

As described in FF and FB equations 29 and 30, Frame based iterative equalizers use FFT-filtering. Thus, in order to express FTNS as a circular convolution to use FFT filtering, Cyclic Extension (CE) should be inserted in the frame and its length should be larger than the channel memory (the vector size of $\mathbf{c}$) to remove inter-block interferences (IBI). In our FTNS scheme, we used Cyclic Prefix (CP), which is a copy of for original frame, for CE.

But as we discussed in 3.2, the FTNS channel vector $\mathbf{c}$ is so large that the required CP length is also large. Thus, the actual size of CP have to be chosen far smaller than the required CP length in order to avoid decreasing spectral efficiency. So we can not avoid IBI in FTNS.

To analyze IBI, let us express $\mathbf{y}$ as a matrix multiplication with $\mathbf{C}$. $\mathbf{C}$ is the circulant matrix of channel vector $\mathbf{c}$ as

$$C = \begin{bmatrix} & & \\ & & \\ & & \end{bmatrix}$$

Figure 16: Circulant matrix of channel vector $\mathbf{c}$

In order to utilize the prior knowledge that the power distribution of $\mathbf{c}$ is symmetric and low-pass shape, we removed the first $N_{CP}/2$ symbols and last $N_{CP}/2$ symbols in the received frame $\mathbf{t}$ to minimize interference energy and get $\tilde{\mathbf{y}}$. This approach does not have any merit in general insufficient CP problem in Nyquist Signaling, because typically the channel is fading channel and its power distribution is not fixed. But in FTNS, both the length and power distribution of $\mathbf{c} = \mathbf{h}_{min} * \mathbf{r}_{\psi\psi}$ are mainly determined by $\mathbf{r}_{\psi\psi}$ which has zero phase response. Thus using the elements around the middle of frame can minimize IBI energy.

Then $\mathbf{y}$ is obtained by circularly shifting $\tilde{\mathbf{y}}$ by $N_{CP}/2$. Similarly, $\mathbf{x}^n$ is also the circularly shifted current block

$$\mathbf{x}^n = [x_{N-N_{CP/2}}, \quad x_{N-N_{CP/2}+1}, \quad \cdots, \quad x_{N-1}, \quad x_1, \quad \cdots, \quad x_{N-N_{CP/2}+1}] \tag{41}$$

And $\tilde{\mathbf{x}}^{n-1}$ and $\tilde{\mathbf{x}}^{n+1}$ are the circularly shifted previous and next blocks. The presence of circular shifts in $\mathbf{y}$, $\mathbf{x}^n$ and $\tilde{\mathbf{x}}^{n\pm1}$ makes interference matrix for us easy to visualize.

$$\mathbf{y} = (\mathbf{C} - \mathbf{\Delta C}) \cdot \mathbf{x}^n + \mathbf{\Delta C}_{up} \cdot \tilde{\mathbf{x}}^{n-1} + \mathbf{\Delta C}_{dn} \cdot \tilde{\mathbf{x}}^{n+1} + \mathbf{w} \tag{42}$$

$$\mathbf{\Delta C} = \mathbf{\Delta C}_{up} + \mathbf{\Delta C}_{dn} \tag{43}$$

$\mathbf{\Delta C}$ is the channel estimation error. $\mathbf{\Delta C}_{up}$ is the interference matrix of the previous frame and $\mathbf{\Delta C}_{down}$ is the interference matrix of the next frame.

$$\Delta C_{up} = \begin{bmatrix} & \blacktriangleleft \\ & \end{bmatrix} \quad \Delta C_{dn} = \begin{bmatrix} & \\ \blacktriangleleft & \end{bmatrix}$$

Figure 17: IBI matrices

The size of non-zero upper and lower triangle sub matrices in $\mathbf{\Delta C}$ are $(N_c - N_{CP})/2$. And $\tilde{\mathbf{x}}^{n-1}$, $\tilde{\mathbf{x}}^{n-1}$ and $\mathbf{x}^n$ are statistically independent to each other.

The way insufficient CP affects the performance of Minimum Mean Square Equalizer (MMSE) on FTNS system was analyzed in [27]. Similarly, the effect of insufficient CP length of our equalizers are tested in this subsection. Compared to previous researches, EST changes signal statistics into a sub-Gaussian distribution. Thus we can simply threat IBI effect as additional AWGN induced at the edge of block.

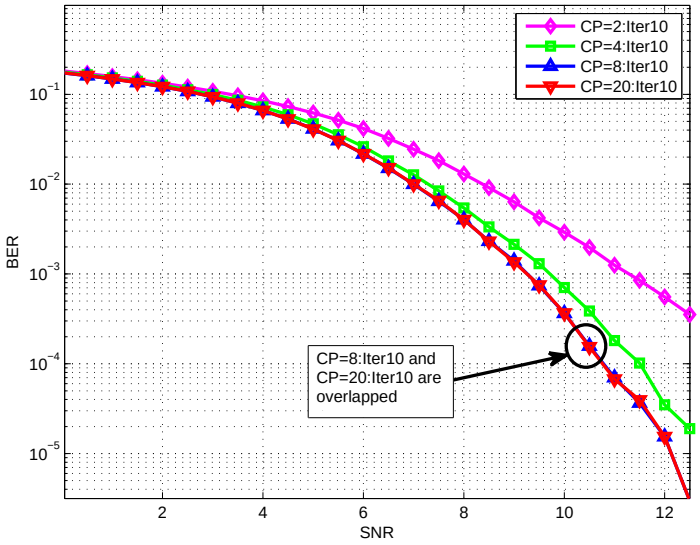

Figure 18: Effect of insufficient Cyclic Prefix: $\rho = 0.8$, $\beta = 0.3$, $\psi(t) \neq 0$ when $t \in [-40\rho T, 40\rho T]$ and $\mathbf{h} = 1$

Figure.18 presents the effect of different cyclic prefix length on EST based FTNS. The channel and modulation scheme is the same as Figure.3. The BER curves converge when CP is 8. Compared to the block size, 2^{12}, 8 is negligible. Therefore the overall spectral efficiency merely reduced by CP in EST based FTNS.

Generally, IBI can be treated as a type of channel estimation error and localized noise. Motivated by the robustness of our equalizer to IBI induced by insufficient CP, we also explicitly simulated in general channel estimation error case without the presence of IBI.

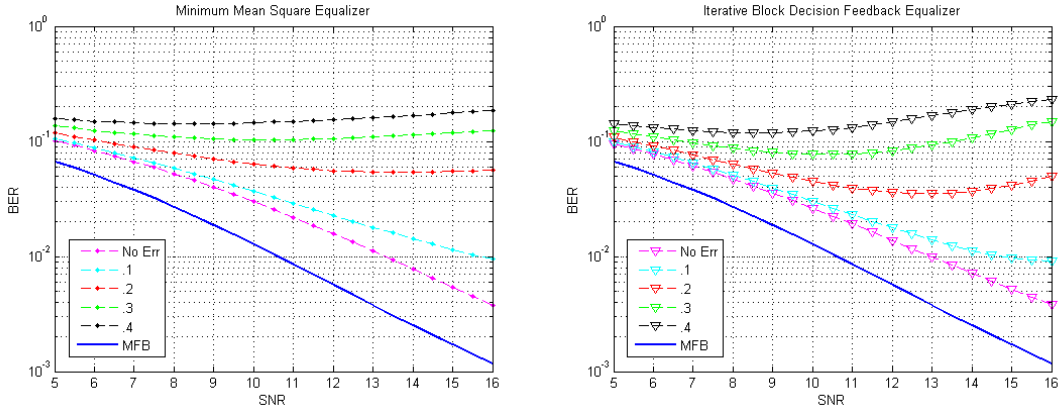

(a) MMSE

(b) IBDFE

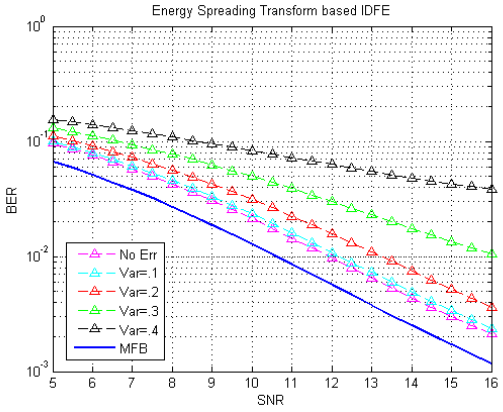

(c) EST based IDFE

Figure 19: Effect of Channel Estimation Error in FTNS : $\rho = 0.8$, $\beta = 0.3$, $\psi(t) \neq 0$ when $t \in [-40\rho T, 40\rho T]$ and $\mathbf{h}$ is a Raleigh fading channel

In figure 19, the channel estimation error $\hat{\mathbf{h}} - \mathbf{h}$ follows Gaussian distribution whose variance is between 0.1 to 0.4. Unlike MMSE and IDFE, BER of EST based IDFE converge in all conditions.

6.3.2 Colored Noise Spectrum / Regularization

Our proposed equalizer in the previous section is numerically unstable in computing FFT frequency bin k around $k \in \left[\lfloor N\rho(1+\beta)/2 \rfloor, \lceil N - N\rho(1+\beta)/2 \rceil\right]$, which are corresponding to the null frequency bands. Because both the noise spectrum W_k and the channel spectrum C_k are oscillating near zero in this region and due the

oscillation, their division can be a huge value. All the other proposed FDE based FTNS schemes we saw in section 3.4 suffer the same problem.

This numerical stability problems of FDE becomes worse when we increase spectral efficiency by changing FTN parameters. This trade-off relationship between the spectral efficiency and the numerical stability are summarized in the table below.

Table 1: Trade off between Spectral efficiency and Numerical Stability

Increasing Spectral Efficiency		Corresponding Results
Decreasing roll-off factor β	$\rightarrow$	Wider null-frequency band
Reducing relative pulse distance, ρ	$\rightarrow$	Wider null-frequency band
Increasing pulse duration $\psi(t)$	$\rightarrow$	More zeros on the unit circle

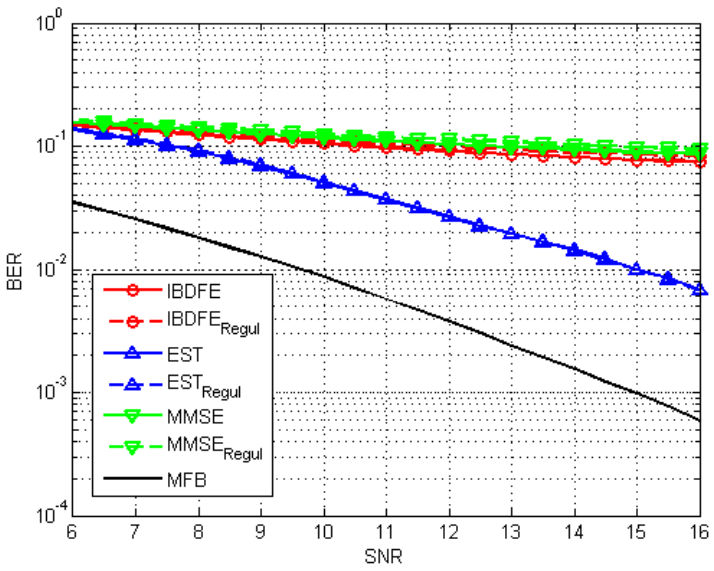

Figure 20: High data rate and poor numerical stability: $\rho = 0.6$, $\beta = 0.2$, $\psi(t) \neq 0$ when $t \in [-60\rho T, 60\rho T]$ and $\mathbf{h}$ is a exponentially decaying Raleigh fading channel

Wider null frequency region introduces more zeros on the unit circle. As the number of zeros on the unit circle increases, the number of oscillations in W_k and C_k spectrum also increase, because noise spectrum W_k is the interpolated sequence of roots of the sampled matched filter $\psi^*(-t)$. Thus, the denominator of FF filter $A_k^{(i)}$ goes to zero and both FF filter and FB filter become unstable.

Figure 20 shows the FTNS performance in ill-conditioned situation. It demonstrates bit-error rate (BER) versus signal-to-noise ration (SNR) under severe FTNS condition: small roll-off factor, β, and a FTN rate, ρ, are long impulse response of $\psi(t)$. Filter **a** and **b** become ill-conditioned due to the high dynamic range of the noise PSD. But as we can see, both regularized and unregularized EST converges while all the others are not.

CHAPTER VII

CONCLUSION

This paper explores efficient and stable Frequency Domain Equalization algorithms for Faster than Nyquist Signaling. FTNS is a way of increasing data rate to maximize spectral efficiency with the expense of additional demodulation complexity. The MLSD type algorithms are suffering high complexity problem. Although FDE algorithms can avoid complexity issues, they have numerical stability problem in FTNS. Furthermore, as spectral efficiency of FTNS increases, these complexity and stability problems become worse. We presented a new FDE based FTNS scheme which is grounded on Energy Spreading Transform based Iterative Decision Feedback Equalizer.

We first investigated Energy Spreading Transform based Iterative Decision Feedback Equalizer by dividing it into two parts: the variations of EST and the variations of IDFE. It was turned out that EST can enhance other IDFE algorithms as well as the IDFE in [17] and its performance is further enhanced by infrequent filter update. Also, we checked that the power of EST is based on the random structure of itself not on the spreading conditions by investigating the performance of ideal-EST.

Then we describe FTNS in a discrete time channel model which our equalizer can be applied to. But due to the long channel response and colored noise of FTNS, we truncated cyclic prefix and reflect noise spectrum into our equalizer scheme.

Insufficient cyclic prefix entails IBI and Channel Estimation error so we tested the robustness of our equalizer. The simulation result showed that our equalizer is robust to both channel estimation error and IBI.

Noise spectrum has null-frequency region which makes equalizer numerically unstable and the null frequency region becomes wider if FTN rate is high. The test result showed that regularization makes our equalizer converges in high FTN rate and the performance gap between regularized and un-regularized scheme is far smaller than other FDE based FTNS scheme.

7.1 Future work

We may extend this thesis two independent way: multi-carrier FTNS, Ideal EST. As we discussed earlier in 3, FTNS can be applied to both time and frequency domain same time. But in that case, the complexity order is increased to $\mathcal{O}(MNlog(MN))$, for 2D-FFT, where M and N are the number of sub-carriers and the time slice in resource block. Because if we the channel matrix $\mathbf{C}$ for vectorized symbol vector is nor sparse (due to the FTNS) neither tridiagonal. So the complexity is bounded to 2D-FFT.

REFERENCES

[1] Anderson, J. B. and Prlja, A., "Turbo equalization and an m-bcjr algorithm for strongly narrowband intersymbol interference," *Proc. Int. Symp. Inf. Theory Appl.*, pp. 261–266, 2010.

[2] Anderson, J. B., Prlja, A., and Rusek, F., "New reduced state space bcjr algorithms for the isi channel," in *IEEE Trans. Commun*, pp. 889–893, IEEE, 2009.

[3] Badri-Hoeher, S., Hoeher, P. A., Chen, H., Krakowski, C., and Xu, W., "Ungerboeck metric versus forney metric in reduced-state multi-user detectors," in *Turbo Codes&Related Topics; 6th International ITG-Conference on Source and Channel Coding (TURBOCODING), 2006 4th International Symposium on*, pp. 1–5, VDE, 2006.

[4] Barry, J. R., Lee, E. A., and Messerschmitt, D. G., *Digital communication*. Springer Science & Business Media, 2004.

[5] Benvenuto, N. and Tomasin, S., "Block iterative dfe for single carrier modulation," *Elec. Letters*, vol. 38, no. 19, pp. 1144–1145, 2002.

[6] Benvenuto, N., Dinis, R., Falconer, D., and Tomasin, S., "Single carrier modulation with nonlinear frequency domain equalization: an idea whose time has comeagain," *Proceedings of the IEEE*, vol. 98, no. 1, pp. 69–96, 2010.

[7] Chan, A. M. and Wornell, G. W., "A class of block-iterative equalizers for intersymbol interference channels: Fixed channel results," *IEEE Trans. Commun*, vol. 49, no. 11, pp. 1966–1976, 2001.

[8] Chan, A. M. and Wornell, G. W., "Approaching the matched-filter bound using iterated-decision equalization with frequency-interleaved encoding," *Proc. of IEEE Globecom02*, pp. 297–301, 2002.

[9] Chen, Q. and Zhang, H., "Shaping filter design for faster-than-nyquist signaling with second order polynomial function," in *Cyber-Enabled Distributed Computing and Knowledge Discovery (CyberC), 2015 International Conference on*, pp. 442–445, IEEE, 2015.

[10] Dinis, R., Montezuma, P., Souto, N., and Silva, J., "Iterative frequency-domain equalization for general constellations," in *Sarnoff Symposium, 2010 IEEE*, pp. 1–5, IEEE, 2010.

[11] Forney Jr, G. D., "Maximum-likelihood sequence estimation of digital sequences in the presence of intersymbol interference," *Information Theory, IEEE Transactions on*, vol. 18, no. 3, pp. 363–378, 1972.

[12] Franz, V. and Anderson, J. B., "Concatenated decoding with a reduced-search bcjr algorithm," *Selected Areas in Communications, IEEE Journal on*, vol. 16, no. 2, pp. 186–195, 1998.

[13] Fukumoto, H. and Hayashi, K., "Overlap frequency domain equalization for faster-than-nyquist signaling," *arXiv preprint arXiv:1509.00562*, 2015.

[14] Gattami, A., Ringh, E., and Karlsson, J., "Time localization and capacity of faster-than-nyquist signaling,"

[15] Hwang, T. and Li, Y., "Novel iterative equalization based on energy-spreading transform," *IEEE Trans. Signal Process*, vol. 54, no. 1, pp. 190–203, 2006.

[16] Hwang, T. and Li, Y., "Optimum filtering for energy-spreading transform-based equalization," *IEEE Trans. Signal Process*, vol. 55, no. 3, pp. 1182–1187, 2007.

[17] Hwang, T., Li, Y., and Sari, H., "Energy spreading transform based iterative signal detection for mimo fading channels," *Wireless Communications, IEEE Transactions on*, vol. 5, no. 7, pp. 1746–1756, 2006.

[18] J. Anderson, F. R. and Owall, V., "Faster-than-nyquist signaling," *Proc. IEEE*, vol. 101, no. 8, pp. 1817–1830, 2013.

[19] Liveris, A. D. and Georghiades, C. N., "Exploiting faster-than-nyquist signaling," *IEEE Trans. Commun*, vol. 51, no. 9, pp. 1502–1511, 2003.

[20] Mazo, J., "Faster-than-nyquist signaling," *Bell Syst. Tech. J.*, vol. 54, no. 8, pp. 1451–1462, 1975.

[21] Prlja, A. and Anderson, J. B., "Reduced-complexity receivers for strongly narrowband intersymbol interference introduced by faster-than-nyquist signaling," *IEEE Trans. Commun*, vol. 60, no. 9, pp. 2591–2601, 2012.

[22] Prlja, A., Anderson, J. B., and Rusek, F., "Receivers for faster-than-nyquist signaling with and without turbo equalization," *Proc. 2008 IEEE Int. Symp. Information Theory*, pp. 464–468.

[23] Rusek, F. and Anderson, J. B., "The two dimensional mazo limit," in *2005 IEEE International Symposium on Information Theory*, pp. 970–974, IEEE Press, 2005.

[24] Rusek, F. and Anderson, J. B., "Constrained capacities for faster-than-nyquist signaling," *IEEE Trans. Inf. Theory*, vol. 55, no. 2, pp. 764–775, 2009.

[25] Sainte-Agathe, F. and Sari, H., "Single-carrier transmission with iterative frequency-domain decision-feedback equalization," in *Signal Processing Conference, 2005 13th European*, pp. 1–4, IEEE, 2005.

[26] Sainte-Agathe, F. and Sari, H., "Iterative frequency-domain decision-feedback equalization," in *Wireless Communication Systems, 2006. ISWCS'06. 3rd International Symposium on*, pp. 1–5, IEEE, 2006.

[27] Sugiura, S., "Frequency-domain equalization of faster-than-nyquist signaling," *IEEE Wireless Commun. Lett.*, vol. 2, no. 5, pp. 555–558, 2013.

[28] Sugiura, S. and Hanzo, L., "Frequency-domain equalization aided iterative detection of faster-than-nyquist signalling," 2014.

[29] Tomasin, S. and Benvenuto, N., "Fractionally spaced non-linear equalization of faster than nyquist signals," in *IEEE Proc. of the 22nd European Signal Process. Conf*, pp. 1861–1865, IEEE, 2014.

[30] Ungerboeck, G., "Adaptive maximum-likelihood receiver for carrier-modulated data-transmission systems," *IEEE Trans. Commun*, vol. 22, no. 5, pp. 624–636, 1974.